CHAPTER 6

Photogrammetry

Ren A. Thompson and Steve P. Schilling

6.1 INTRODUCTION

Since its conception over a century ago, photogrammetry has been a mathematically rigorous cartographic tool for extracting geodetic information from stereo photography. Defined by the American Society of Photogrammetry as '*the science or art of obtaining reliable measurements by means of photography*' (Whitmore, 1952), photogrammetry provides the foundation for many standard cartographic datasets that serve as tools in the volcanologist's kit, including topographic maps, orthophotographs, digital elevation datasets, geologic maps, and infrastructure maps. With the advent of high-speed microprocessors, real-time GPS systems (Chapter 4), and the growing availability of satellite-imaging systems, photogrammetry has evolved from dedicated photogrammetric mapping venues to portable modular applications that can be readily integrated with other systems to provide near real-time, 3-D mapping and monitoring capability over large areas.

Despite recent technological developments, the fundamental principles of photogrammetry and the basic requirements for developing successful applications remain unchanged. As noted in the Preface and Chapter 1, volcanologists charged with assessing unrest at volcanoes are often faced with the challenge of implementing field-based monitoring systems that require innovative and often unconventional solutions to complex problems. Understanding the basic principles of photogrammetry enables them to tailor photogrammetric tools to a broad range of applications and geologic situations.

Wolf (1983, p. 159) provides the following useful introduction to the phenomenon that lies at the heart of photogrammetry (i.e., *stereoscopic parallax*). Hold up a finger in front of your face and alternately blink your eyes while focusing on the finger. This is *not* a test of mental or physical acuity – please bear with us for a moment. Your finger will appear to move from side to side with respect to objects beyond it, such as the pages of this book. The closer the finger is held to the eyes, the greater will be the apparent shift. No one is looking – try it!

Conceptually, photogrammetry is the mathematical formulation of the procedure that your eye–brain combination uses to determine the distance from your eyes to your finger or any other object. The shift in apparent position is related to the angular separation between your eyes at the distance in question, which is called the *parallactic angle*.[1] The average person, with an eye separation of about 66 mm, is capable of discerning parallactic-angle changes of about 3 seconds of arc. This corresponds to distinguishing range differences of about 4 m at 100 m – pathetic by raptor standards, but mostly adequate for *Homo sapiens*.

6.2 HISTORICAL PERSPECTIVE

The application of geologic photogrammetry to volcano geodesy has its roots in the development

[1] The parallactic angle, also known as the convergence angle, is formed by the intersection of the left eye's line of sight with that of the right eye. The closer this point of intersection is to the eyes, the larger the parallactic angle. As the eyes scan overlapping areas between a stereo image pair, the brain receives a continuous 3-D impression of the ground. This is caused by the brain constantly perceiving the changing parallactic angles of an infinite number of image points making up the terrain. The perceived 3-D model is known as a stereoscopic model (Section 6.3.6).

D. Dzurisin, *Volcano Deformation*

of modern photography and cartography. The popularity of photography and stereoscopy in the second half of the 19th century provided the impetus to apply this emerging technology to cartographic applications. In 1855, Nadar (Gaspard Félix Tournachon) obtained the first aerial photographs from a balloon about 80 m above the ground. Aerial photography was used during the American Civil War (1861–1865) and Franco–Prussian War (1870–1871) for purposes of military reconnaissance. Concurrently, the effects of lens distortion in cartographic applications became known, and techniques were devised to both reduce distortion and mitigate its consequences. However, not until George Eastman developed the nitrocellulose film base in 1885 and the Wright brothers pioneered the airplane in 1903 did the two critical elements of early photogrammetry materialize in a way that enabled collection of stereo imagery over large areas suitable forcartographic applications. Consequently, photographic film became the first remote-sensing medium utilized in the production of maps and for other applications in geology (Ray, 1960; Sabins, 1999).

The first half of the 20th century witnessed the development of a number of stereoplotting instruments (i.e., instruments to view adjacent overlapping photographs and make measurements) designed to facilitate the quantitative production of maps and geodetic measurements from stereo aerial photographs, along with development of cameras specifically designed for aerial photography. The derivation of rigorous mathematical formulas constraining the resection, orientation, rectification, and scaling of imagery in the 1920s and 1930s quickly led to the development of both analog and analytical instrumentation for stereoscopic mapping during the remainder of the 20th century. Subsequent commercialization of the photogrammetry industry evolved around the ever-increasing demand for photography and instrumentation capable of higher accuracy and output. By the 1960s, topographic mapping based on photogrammetry was employed worldwide for national-scale programs. Geologic applications including geologic mapping, geomorphic change studies, and landslide and volcano monitoring became common by the mid-1970s through 1980s. Fully automated digital-photogrammetric systems were introduced in the 1990s, and today the range of possibilities is limited only by the availability of high-quality stereo photography and geodetic control with which to orient the imagery to real-world coordinate systems. Even this last requirement is easing, as both aerial and handheld cameras with on-board Global Positioning System (GPS) receivers (Section 4.3) can alleviate or minimize the need for external ground control in many situations. The growing advantage to the volcano community is that photogrammetric applications which, in the past, took days to weeks to execute, are now possible in near real-time and with a relatively modest investment in equipment.

6.3 PHOTOGRAMMETRY FUNDAMENTALS

6.3.1 Introduction

Photogrammetric applications in geology can be classified as either aerial or terrestrial, based on whether the photography was collected from aerial or ground-based cameras. Traditionally, both approaches have focused on extraction of geologic information from photographs collected specifically for the purpose of reconstructing a distortion-free stereoscopic terrain model – one of several applications of direct interest to volcanologists. The geometric requirements for collection of photography in both approaches are identical, although aerial photography is more widely available and instrumentation required for extraction of quantitative data from aerial photography is far more accessible than that required for terrestrial imagery. Additionally, aerial photography is widely available covering a broad range of nominal scales and is well suited to rigorous geologic and topographic mapping, as well as reconnaissance or 3-D terrain analysis over large areas. Generally, terrestrial applications are more aerially restricted and site-specific. The basic elements of aerial photogrammetry are outlined below; terrestrial photogrammetry is addressed in Section 6.6. More detailed treatments of these subjects can be found in Wolf and Dewitt (2000), American Society for Photogrammetry and Remote Sensing (1997), and references therein.

Nearly all imagery collected for photogrammetric analysis is based on electromagnetic energy with wavelengths within the visible (0.4 to 0.7 mm), ultraviolet (0.3 to 0.4 mm), and near infrared (0.7 to 1.2 mm) portions of the spectrum (Figure 6.1). If an object reflects all wavelengths of visible light, it will appear white to the human eye or film emulsion; conversely, if it absorbs all wavelengths it will appear black. If an object or surface absorbs all visible blue

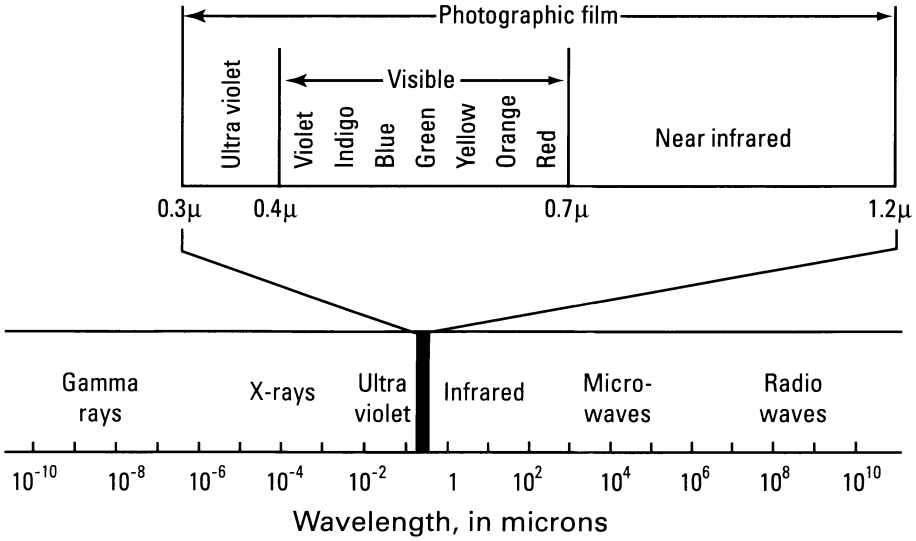

Figure 6.1. Simplified classification of the electromagnetic spectrum by wavelength. Most photographic and photogrammetric applications make use of the visible, near infrared, and ultra violet part of the spectrum (expanded portion).

and red wavelengths it will appear green, and likewise for other wavelength combinations within the visible spectrum. Film emulsions used in photogrammetry have been optimized for sensitivity to certain parts of the electromagnetic spectrum depending on the intended application. For example, black and white emulsions are sensitive to blue and ultraviolet energy; color or panchromatic emulsions are sensitive to red, green, and blue wavelengths. Color infrared emulsions record images in the near-infrared part of the spectrum, beyond what is visible to the human eye. By far, the most common applications in geology utilize conventional black and white emulsions because of their wide availability, low cost, and high resolution. True-color emulsions are reserved for applications in which rendering natural scenes as accurately as possible is a high priority.

6.3.2 Aerial cameras

Cameras used for collection of aerial photographic images are classified as either *film* or *digital*. Film cameras record images by focusing reflected electromagnetic radiation, predominantly visible light rays, on silver-halide film emulsions. Digital cameras employ *charge coupled devices* (CCDs) to measure the intensity of light exposed on a matrix of picture elements (pixels). Each element builds up an electric charge proportional to the incident light energy received and represents this as a tonal value for each pixel in a digital photograph. Digital-imaging technologies are relatively new in the field of photogrammetry and acquisition of digital images collected with digital cameras is rare. Far more commonly, film-based aerial photographs are digitally scanned as needed for digital applications. A discussion of digital-scanning applications is presented in Section 6.4.

Film cameras can be subdivided further into fixed-frame and scanning varieties. Fixed-frame cameras are more common and expose a single image frame on film with each opening of the camera shutter. Scanning cameras typically employ a rotating lens element to focus collimated light rays along predefined paths or rows of the film plane, progressively exposing the entire image after multiple passes. They come in many different geometric configurations and are largely restricted to special purpose applications. The single lens, fixed-frame aerial camera remains the mainstay of geologic and cartographic applications in photogrammetry.

In addition to being extremely precise and expensive instruments, all single lens, fixed-frame cameras used in aerial photography, regardless of manufacturer, share several common attributes. Modern camera lenses employed in the manufacture of aerial cameras represent the epitome of the optical lens-makers craft. Each is characterized by extremely high resolving power and minimal to virtually non-existent lens distortions – two features that are critical to using aerial photography for quantitative, 3-D measurements. Since the lens-to-object distance is large relative to the typical focal

length of the lens, fixing the focus at infinity enables optimum optical performance and simplifies lens construction and calibration.[2]

To capitalize on the optical integrity of the lens, the lens-mounting system and camera body must be rigid and maintain precise geometry such that the lens axis is as nearly perpendicular as possible to the film plane in the camera body. As film-based photographic emulsions are inherently flexible, all modern aerial cameras utilize some form of film stabilization system. The most common type is a vacuum system in the film chamber that activates immediately prior to release of the camera shutter, pulling the film perfectly flat against the film backing plate. The vacuum is released prior to advancing the film to the next frame using a motorized, high-capacity film magazine capable of holding enough film rolls to capture hundreds of exposures.

6.3.3 Format, focal length, and field of view

Stereoplotters, instruments that are used to orient overlapping aerial photographs, are designed to work with imagery at the scale of the negative produced by the camera/lens combination. Consequently, most aerial cameras utilize large film formats, typically 230 mm (9 in) square. The focal length of an aerial camera using the 230 mm-square format determines the field of view recorded in each image. By far, the most common focal length used today is 152 mm (6 in), with an angular field of view of 94°. This is considered a wide-angle lens and yields suitably large image footprints for many applications. The relationship between angular field of view, lens focal length, and film format is:

$$\theta = 2\tan^{-1}(d/2f) \qquad (6.1)$$

where θ is the lens angular field of view, d is the diagonal distance across the film frame, and f is the lens focal length. For a 230 mm film camera using a 152 mm lens, the angular field of view is:

$$\theta = 2\tan^{-1}\left[\frac{\sqrt{(230^2 + 230^2)}}{2(152)}\right] = 94^\circ$$

Aerial camera lenses are classified on the basis of their angular field of view as super wide-angle ($\theta \geq 100^\circ$), wide-angle ($\theta = 75$–100°), or normal ($\theta \leq 75^\circ$). Less common, but still used, are lenses with focal lengths of 89 mm (3.5 in), 210 mm (8.25 in), and 305 mm (12 in), which have angular fields of view of 123°, 76°, and 56°, respectively. Examination of (6.1) reveals the inverse relationship of focal length to field of view (i.e., as the focal length increases, the field of view decreases). Consequently, the image footprint decreases with increasing focal length for the same flight height. Lenses with focal lengths significantly shorter or longer than 152 mm are used mostly for unusually low- or high-altitude photo missions, respectively.

6.3.4 Photo collection and scale

Aerial photography for mapping and monitoring applications is typically classified as vertical or oblique, depending on the orientation of the camera relative to the ground surface. In the case of vertical aerial photography, the goal is to maintain an orthogonal orientation of the camera-lens axis relative to the ground surface. For oblique aerial photography, the camera axis can be oriented at high to low angles relative to the ground surface (i.e., near-vertical to near-horizontal), depending on the application. An important consideration for aerial photo collection in volcanic terrain is the need for combining vertical and oblique aerial photography to optimize image resolution in areas of high relief or intense shadowing resulting from less than ideal sun angles. Partial obscuring of the ground surface by clouds or volcanic fume can also be a problem. Often these difficulties can be circumvented by combining hand-held photography, typically collected from a light aircraft or helicopter, with conventional vertical aerial photography. In either instance, strips of photos are collected at the same altitude, with each successive photo overlapping its predecessor by approximately 60%. Adjacent parallel strips are collected while maintaining approximately 20–30% side overlap with the previous strip (Figure 6.2). In this manner, large areas can be collected in a single

[2] Careful calibration of aerial cameras and lenses is essential to achieving the best possible photogrammetric precision. Clarke and Fryer (1998) provide a thorough discussion of the development of calibration methods and models, which includes the following introduction (p. 58): *'A camera consists of a image plane and a lens which provides a transformation between object space and image space. This transformation cannot be described perfectly by a perspective transformation because of distortions which occur between points on the object and the location of the images of those points. These distortions can be modelled. However, the model may only be an approximation to the real relationship. How closely the model conforms to reality will depend on the model and how well the model's parameters can be estimated. Choosing parameters which are both necessary and sufficient has taxed those involved in the process of lens calibration for as long as lenses have been used to make precise measurements.'*

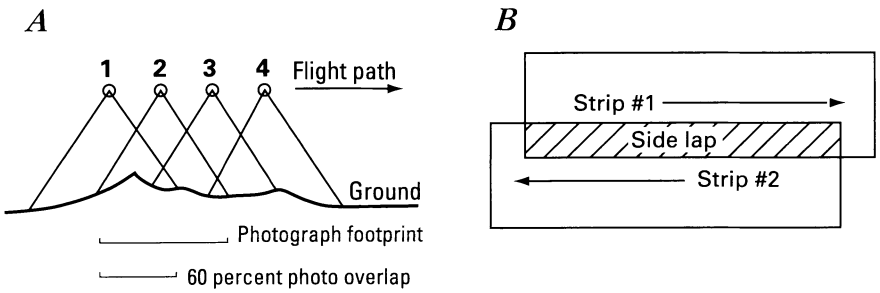

Figure 6.2. Geometric representation of aerial photography collected with 60% overlap in sequential photos (A) and 20–30% overlap for adjacent photo strips (B).

flight while maintaining the photo geometry necessary for stereo rectification.

The nominal *photo scale*, or ratio of the unit length measured on the photo to the equivalent distance represented on the ground, is a function of the height of the camera platform above the ground surface and the focal length of the camera lens:

$$S = f/H = 1/(H/f) \qquad (6.2)$$

where S is the scale, f is the focal length, and H is the camera flight height. Both f and H are expressed in the same units, typically feet, meters, or millimeters. H represents the nominal camera height above the ground, usually determined by the aircraft altimeter. For example, photos taken with a 152 mm lens at an altitude of 3,648 m would have a scale represented by: $Scale(S) = 1/(3,648/0.152) = 1/24,000$, more commonly written 1 : 24,000. Figure 6.3 shows aerial photos flown over Mount St. Helens on 25 September 2000, at nominal scales of 1 : 24,000 and 1 : 12,000, using the same camera with a 152 mm focal length lens flown at nominal altitudes of 3,648 m and 1,824 m above the 1980–1986 lava dome surface, respectively.

The horizontal scale of aerial photographs can vary significantly across the field of view, depending on the vertical relief of the ground surface. Any departure from a flat surface effectively changes the camera flight height (H) in (6.2), which affects the scale in the photographs. For the photo shown in Figure 6.3, for example, point A on the crater floor of Mount St. Helens lies at an elevation of approximately 2,000 m above sea level and point B on the crater rim is nearly 450 m higher. As a result, the scale in the photo varies from 1 : 24,000 at A to 1 : 21,039 at B (assuming a nominal flight height of 3,648 m above the 1980–1986 dome or 5,648 m above sea level). Commonly, aerial photographs flown for both commercial and geologic purposes include the average photo scale and the precise focal length of the camera lens on the film negatives for each project.

Most aerial photography flown for purposes of monitoring deformation or other surface change at active volcanoes is specifically targeted at resolving objects at a given photo scale. Typically, this might be a control-point tower or air-photo panel, a series of visually identified landmarks used as control points, or even a geomorphic landform such as a lava dome or flow. Owing to the variation in scale that can occur across a single image in regions of high terrain relief, substantial care must be taken to ensure sufficient stereo overlap at the required scale for image interpretation. Examples of the potential for omission of critical data are illustrated in Figure 6.4.

6.3.5 Relief displacement

Relief displacement occurs in all vertical aerial photographs as a result of the perpendicular orientation of the camera axis relative to the ground surface. This results in objects, trees for example, that appear to lean away from the *principal point*, or optical center of the photograph. The amount of relief displacement in any given photo is directly proportional to the height of the object and its distance from the principal point of the photo, and is inversely proportional to the flight height above the object. The practical consequence of this phenomenon is that areas of high relief, photographed at relatively low altitude, are typically subject to large amounts of relief displacement. This relief displacement, coupled with variable scale typically observed in these photographs, results in images that require rectification before they can be used to make quantitative measurements. This type of rectification differs significantly from mathematical transformations or digital rubber-sheeting techniques that serve to locally adjust photo-image coordinates to accommodate local cartographic ground control. Such methods work reasonably well for photographs with

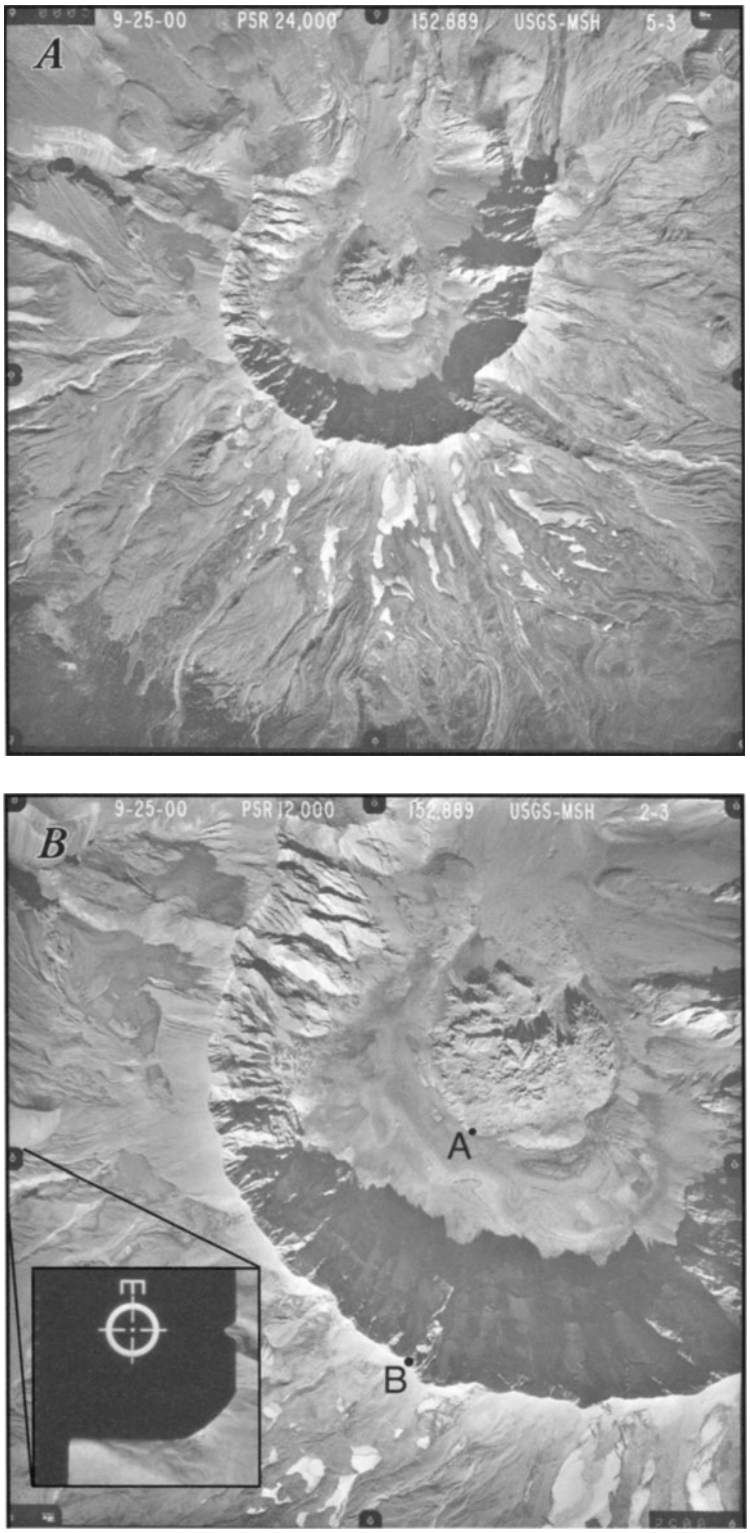

Figure 6.3. Aerial photographs of the crater and lava dome of Mount St. Helens taken in September 2000 at nominal scales of 1 : 24,000 (A) and 1 : 12,000 (B), the latter reproduced at 50% of original scale. See text for discussion of points 'A' and 'B' in the bottom image. Note camera focal length (152.889 mm) at top of each photo. Inset in bottom image shows enlarged view of left center fiducial mark. Similar marks occur in all four corners and at the center of each edge of all aerial photographs. The exact configuration and style of fiducial marks varies from camera to camera.

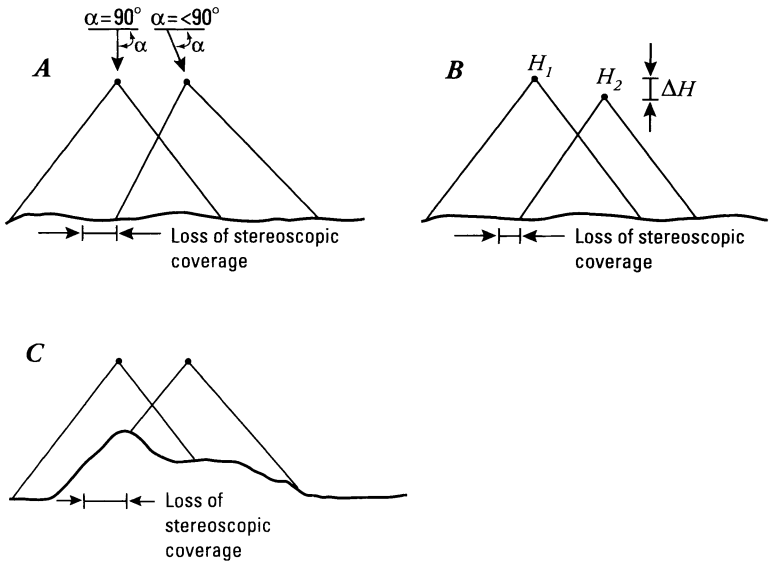

Figure 6.4. Circumstances preventing the degree of stereo coverage required for photogrammetric rectification include unanticipated camera axis rotation such that $\alpha < 90°$ (A), fluctuation in altitude where $(H_1 - H_2) = \Delta H$ (B), or severe variation in topographic relief between adjacent photos (C).

minimal scale variation and low relief, but produce unacceptable levels of distortion when applied to photographs of high- or variable-relief volcanic terrain. In such cases, preparation of an *orthophoto*, or rectified photographic image, is needed to extract quantitative 2-D image information, and stereomodel orientation is required to obtain 3-D information. Both of these techniques require photogrammetric instrumentation for proper orientation of aerial photographs prior to analysis.

6.3.6 Orientation

A photogrammetric instrument called a stereoplotter is used to reconstruct a distortion-free stereoscopic model of the ground surface. In such a model, points, lines, and surfaces can be constructed in 3-D space and projected in 2-D as needed for map or orthophoto preparation. Modern orthophoto production requires digital photogrammetric instrumentation (Section 6.4), but relies fundamentally on techniques developed for analog, or opto-mechanical stereoplotters, for image rectification.

Any two overlapping photographs of an aerial strip can be viewed in stereo, providing a 3-D visual image of the ground surface. Such a pair of photos is referred to as a *stereo model*. There are typically many stereomodels depending on the length and number of flight strips associated with the photo mission. Each image of the stereo model can be thought of as a series of bundled light rays representing the fixed geometry of the reflected electromagnetic radiation from the ground surface relative to the camera in the aircraft. For the overlapping 60% of adjacent photographs, two such bundles of light rays are represented for each model. For each stereo model, a 3-D image of the terrain can be reconstructed from the two photographs by knowing the relative position and rotation of the camera lens for each photograph. To create the stereo model, modern analytical and softcopy stereoplotters use mathematics to reconstruct the geometry of the original light paths relative to the camera, taking into account known quantities such as photo-flight parameters and characteristics of the aerial camera system. For our purposes, the geometric constraints involved are better illustrated by reference to mechanical (analog) stereoplotters.

Photogrammetric *orientation* of stereo images is basically the same for both aerial and terrestrial photography, and is divided into three steps: interior orientation, relative orientation, and absolute orientation. All three orientations must be performed to establish photogrammetric and geodetic rectification.

Interior orientation involves establishing the geometric configuration of the camera relative to the film image. To re-establish the path of light for any point on the film image, the projection center and focal length of the camera/lens combination used to collect the photographs must be known. These parameters are readily available in the form of a

calibration report for aerial cameras used in most aerial applications. Often the camera focal length is recorded as a notation directly on the film image, and information about the projection center can be derived indirectly from the aerial photos. *Fiducial marks* are recorded on the border of each photo, typically one on each side and one in each of the four corners (Figure 6.3(B)). The intersection of lines connecting opposite fiducial marks is called the *center of collimation*. This is an important point of reference for photogrammetric measurements. For an ideal camera/lens combination, the center of collimation is coincident with the photo principal point (i.e., the intersection of the film plane and the lens projection center). Hereafter, we assume this to be the case, and refer simply to the principal point. Fiducial marks are characteristic of the aerial camera; the lens projection center and focal length are determined by repeated calibration throughout the life of the camera.

Relative orientation re-establishes the photo positions for the stereo model and, consequently, the ray paths for adjacent photos established during photo collection. One way to accomplish this is to physically position the photographs next to each other and re-establish the ray paths for each photograph relative to the same points in space. Assuming the position of one photograph is fixed in space, the second photograph has six degrees of freedom with respect to the first. Three of these parameters are translations along the x, y, and z axes, and the other three are rotations about the same axes (Figure 6.5). The translation bx is along the flight line, by is orthogonal to the flight line, and bz is along the vertical axis. The rotations ω, ϕ, and κ, are around the x, y, and z axes, respectively.

For any two photographs for which the ray paths have been reconstructed, a translation in the direction of flight bx influences scale changes between photos but not the intersection of light rays from adjacent photos; therefore, such translations are not considered in the orientation procedure. However, all five of the remaining translations are treated as unknowns and must be determined such that five pairs of light rays intersect when positioning the second photo relative to the first. A displacement in the y-axis direction by results in non-intersection of light rays for all five pairs of light rays for adjacent photos. This by translation, or y-parallax, is removed during the relative-orientation process by making iterative and diminishing adjustments to by, bx, ω, ϕ, and κ for one photo relative to the other. In opto-mechanical stereoplotters, these

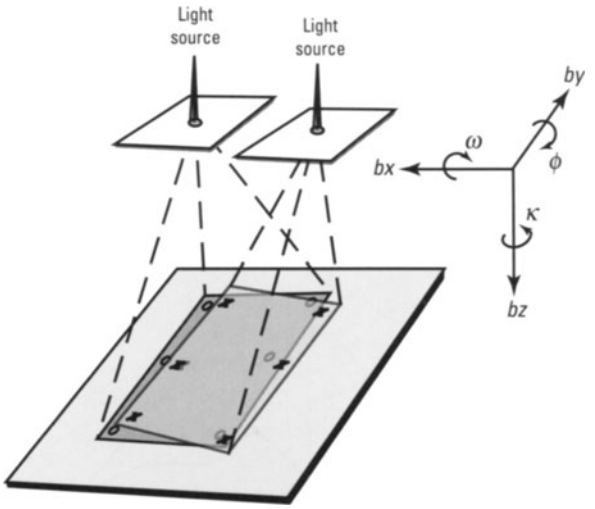

Figure 6.5. Diagrammatic representation of the three translations and rotations about the x, y, and z axes relative to the projected view of the overlap area on a single stereo pair.

adjustments are made physically by moving of one photo relative to the other using both translations parallel to, and rotations about the x, y, and z axes. In analytical and softplotter systems, the same problem is solved mathematically. In both cases, the solution converges toward the same relative orientation that existed when the photos were acquired.

The implementation of translations for removing y-parallax varies from instrument to instrument, but follows the same basic procedure (Figure 6.6). The five pairs of light paths for adjacent photos intersect at points 1 through 5 for a properly oriented stereo model. Although the actual positions of the points in the model are arbitrary, the relative position and the numbering system used have become industry standards. A relative orientation starts by removing the y-parallax in point 1 by means of a by translation.

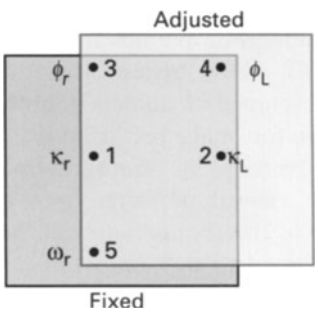

Figure 6.6. Effect of iterative adjustment of translations and rotations on one photo in a stereo pair relative to the fixed photo during a relative orientation. See text for discussion.

Next, the parallax in point 2 is removed without adversely affecting the orientation of point 1. A rotation about the z-axis, κ, centered at point 1 will remove the parallax from point 2. The y-parallax in point 3 is removed by a translation along the z-axis, bz. This introduces an x-parallax at point 2, which can be removed later by proper scaling, but does not introduce y-parallax at points 1 and 2. The y-parallax in point 4 is removed with a translation ϕ, again not introducing any significant new parallax to points 1, 2, and 3. Finally, to remove the y-parallax in point 5 we introduce a translation ω about the axis of the flight line. This translation introduces y-parallax in previously adjusted points 1 through 4, which must be revisited. The iterative procedure continues until parallax is minimized at points 1 through 5 and, consequently, at all points in the stereo model. The impact of adjusting one parameter on the relative position of points within the model is illustrated in Figure 6.7.

Precise 3-D measurements can be made from the stereo model once a suitable relative orientation has been established. However, the model is not oriented and scaled to a geodetic coordinate system (i.e., to the real world) until ground-control information is included. This is done mechanically for analog systems and mathematically for analytical and softcopy instruments.

Absolute orientation allows the model, cleared of all distortion, to be precisely oriented in space so that 3-D coordinate measurements (x, y, z) in the model can be transformed to ground coordinates in a geodetic coordinate system. The absolute orientation, like the relative orientation, is an iterative process involving solution for seven unknown parameters: scale (S), three linear translations (x_o, y_o, z_o), and three angular rotations (ω around the x axis, ϕ around the y axis, and κ around the z axis).

Solving for these seven parameters requires seven independent pieces of information about the precise location of the aerial camera. The most sophisticated aerial camera systems have inertial platforms that record, at the instant of exposure, the camera rotations (ω, ϕ, and κ) and precise camera coordinates using sophisticated GPS systems. Together with the flight altitude, this theoretically provides all the information necessary to solve for the seven unknowns. Unfortunately, these systems lack sufficient precision or accuracy to provide a real-time solution completely independent of external GPS ground control. Nonetheless, they can reduce the amount of ground control required to solve the external orientation by nearly an order of magnitude. Lacking information about camera orientation and position, an exterior orientation can be performed using ground control points (i.e., points of reference visible in the model that have known geodetic control positions).

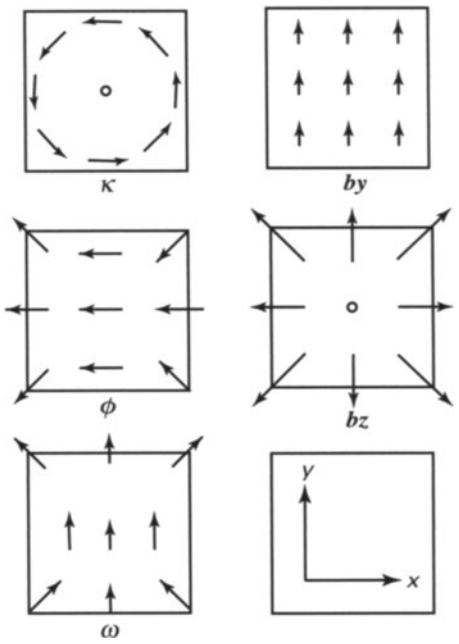

Figure 6.7. Iterative adjustment sequence and the impact of adjusting each parameter on the relative positions of points during a relative orientation of a stereo model. See text for discussion.

The minimum amount of ground control required to orient a stereo model is two horizontal points (x and y coordinates) and three elevation points (z coordinates). These need not be the same points, but the horizontal and elevation requirements can be combined such that two of the required elevation points can be horizontal control points as well. The distribution of control points within the area of stereo overlap determines the accuracy of the orientation outside the area encompassed by the control points. For best results, elevation points should form a large triangle and the (x, y) coordinate pairs should be separated as far as possible (Figure 6.8).

A standard spatial coordinate transformation is used in analytical and softcopy stereoplotter systems to perform the absolute orientation. This method can be illustrated geometrically and described relative to the physical parameters required for the orientation. This method only works for models having minimal tilts, typically less than 1°. This requirement is met for the majority of aerial photographs, making these photos well suited to analysis

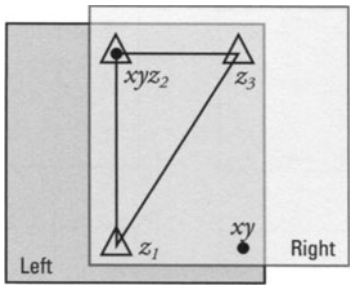

Figure 6.8. Relative positions of representative control points necessary to rectify a single stereo model during an exterior orientation. *x* and *y* are horizontal coordinates; *z* is the vertical coordinate.

with analog instruments. On the other hand, most hand-held aerial and terrestrial photographs have variable tilts exceeding several degrees, which requires spatial coordinate transformations that can be accomplished with analytical and softcopy photogrammetric systems.

The model scale is calculated by comparing the distance L on the ground to the same distance l in the model. This is expressed as:

$$l = \sqrt{(x_2 - x_1)^2 + (y_2 - y_1)^2} \qquad (6.3)$$

where the x and y coordinates are known horizontal control positions. The scale for the absolute orientation is:

$$S = l/L \qquad (6.4)$$

The rotation about the z-axis (κ) is determined by comparing the azimuth between the two plane ground control points and the azimuth between the same points measured in the model. The translation is calculated as:

$$\kappa = Az_t - Az_m \qquad (6.5)$$

where Az_t and Az_m are the azimuths of the ground control points on the Earth and the photo model, respectively. Once the scale and the κ translation are determined, the ground distances between the three elevation points are determined by multiplying the model distances by the scale. Subsequently, the ω and ϕ translations are determined in a similar way.

For purposes of illustration, consider the case in which two of the three elevation points (z_1 and z_2) lie along a line in the model y-axis, and the third point (z_3) forms a line with z_2 along the model x-axis (Figure 6.8). The translation ω is determined by:

$$\omega = \arctan((z_{lm} - z_{lt})/l_{12}) \qquad (6.6)$$

The translation ϕ is likewise determined from elevation points z_2 and z_3 by:

$$\phi = \arctan((z_{3m} - z_{3t})/l_{23}) \qquad (6.7)$$

Obviously, real-world situations would dictate more complicated geometry for the location of control points, but the geometric solutions remain similar, albeit more complex.

After determination of the scale and three rotations (ω, ϕ, and κ), the linear transformations (x_o, y_o, z_o) are determined simply by subtracting the rotated-and-scaled model coordinates from the known ground coordinates for the horizontal control points. Once the absolute orientation of the model is completed, points from one model can be transferred to an adjacent photo and used as control in the orientation of the second model. This generally works well, as long as the control points being transferred are easily identified in the adjacent photo. Two of the ground control points required to orient the second model can be transferred from the first model, requiring only one additional elevation control point for absolute orientation. In practice, using three or more control points in the overlapping part of the model ensures sufficient control for statistical analysis of error associated with the orientation. The procedure can be continued for orientation of an entire strip of models with the understanding that any orientation or control-point errors present early in the process will be propagated throughout the length of the strip.

6.3.7 Photogrammetric accuracy

Photogrammetric accuracy based on a properly oriented model is determined primarily by the quality of the instrumentation used and the quality of the photographic film. Individual points can typically be collected with an accuracy of about 10 microns at the film scale on analog stereoplotters, and down to 3 microns on high-end analytical stereoplotters. This translates to ground units by multiplying the instrument accuracy by the scale of the photographs. In practical application, only the most experienced operators are capable of realizing accuracies close to those possible with modern instruments. However, even inexperienced users are routinely capable of making measurements with accuracies of 20 microns at the film scale, or ~0.5 m on the ground, using 1 : 24,000-scale photography. This is adequate for most geologic mapping applications, but might not be sufficient for deformation monitoring.

It is important to distinguish relative accuracy from absolute accuracy in photogrammetric projects. Relative accuracy is the accuracy of measuring two points relative to each other in a single stereo model. In this case, the previous discussion of accuracy applies. Absolute accuracy refers to the accuracy of measured model points relative to a geodetic coordinate system. The degree to which the absolute accuracy approaches the relative accuracy is determined by the quality of the ground control used in the absolute orientation of the stereo model.

In most photogrammetric applications in geology, the quality of the ground control is the weak link in the orientation process. In many remote areas of the world, high-quality geodetic ground control is limited in extent and availability. Existing topographic maps often provide the only ground control for orientation purposes, unless allowances are made for collection of GPS or conventionally surveyed control. When GPS or survey control is unavailable, cartographic features on the topographic map such as road or stream intersections that can also be identified in the photographs are used for the absolute orientation. Unfortunately, the cartographic uncertainties associated with the original map production might be unknown, which severely limits the absolute accuracy of the photogrammetric project. If full photogrammetric accuracy is required, ground control measurements must be accurate to the same order as the relative or theoretical accuracy of the photogrammetric instrumentation.

6.4 INSTRUMENTATION AND DATA TYPES

Photogrammetric instrumentation falls into three classes, which share common requirements for orientation of stereo aerial photographs, including interior, relative, and absolute orientation for quantitative image rectification. To a degree, all three also share common ergonomic controls for data collection. Beyond adherence to the fundamental principals of photogrammetry, the three classes of instrumentation vary dramatically in capability and utility for geodetic application at volcanoes. Brief descriptions of each class are provided below with an emphasis on fundamental characteristics, advantages, and limitations inherent in each design. For a more thorough treatment of the historical context, mechanical construction, and theoretical design characteristics of stereoplotters, the reader is referred to Wolf and Dewitt (2000) and references therein.

6.4.1 Analog stereoplotters

Analog stereoplotters are characterized by coupled optical and mechanical systems designed to replicate precise geometries linking object points on the ground to the orientation of stereo aerial photographs at the precise moment of acquisition. With properly oriented photographs, these instruments enable 3-D acquisition of coordinate data, facilitated either by digital encoders corresponding to the x, y, and z coordinate axes or by projection, typically through use of a mechanical pantograph, onto 2-D base materials. Historically, the primary application of analog instruments was for topographic mapping, but these instruments were easily adaptable for geologic map compilation. Largely displaced by analytical and softcopy stereoplotters for topographic mapping, analog instrumentation is still commonly used for geologic applications.

A stereo pair of diapositives (positive images on a transparent medium, usually polyester film or glass) or paper prints is oriented so light projected through, or reflected from, the images produces bundled light-ray paths such that intersecting light rays of the same object point on the left and right images form a stereo model (Figure 6.9). This viewing geometry corresponds to the inverse of the angular geometry experienced during the in-flight acquisition of the same stereo pair. Analog stereoplotters developed largely during the 1960s and 1970s shared common characteristics, including an optical viewing system, a measuring and tracing system, and a reference or tracing table (Figure 6.10). The mechanical carriage and optical-viewing systems of analog stereoplotters are designed to facilitate the range of motions necessary to perform interior and relative orientations of individual stereo models (Section 6.3), while maintaining an optical-viewing path that provides sufficient magnification for photo interpretation and visual confirmation of stereo superposition. Most analog systems employ: (1) overhead carriage-mounted photographs; (2) high-quality binocular viewing systems directed upward toward the illuminated left and right images; and (3) mechanical, hand-operated tracing stands for simultaneously moving the optical train through the region of stereo overlap on the photos and for adjusting

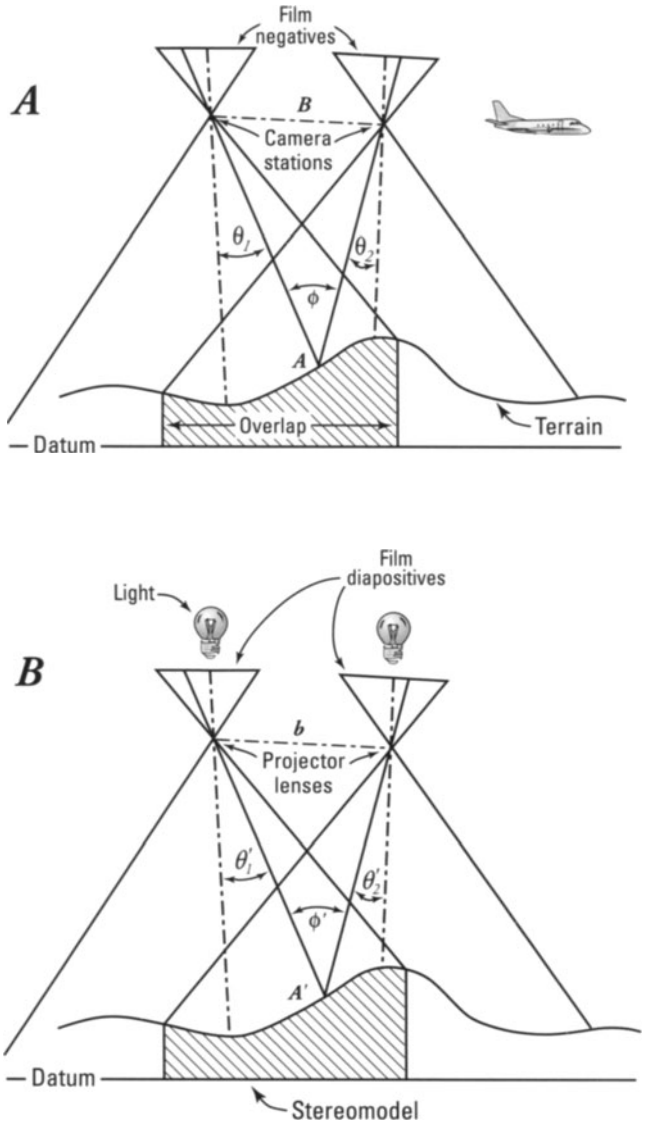

Figure 6.9. Geometric configuration of camera stations and aerial photograph negatives relative to the ground surface (A), and equivalent geometry established in an analog stereoplotter for diapositive images (B). The stereoplotter orientation ensures that original camera positions, distances (B, b), and ray path angles (ϕ, θ_1, θ_2) and ($\phi', \theta'_1, \theta'_2$) are related by the model solution (modified from Wolf and Dewitt, 2000).

the relative positions of the photos to maintain stereo viewing. A floating mark, or narrow beam of projected light, is superimposed on the center of the optical path for both left and right images. A rotating wheel on the tracing stand is adjusted until identical points on each photo, representing a single position on the ground, occupy the same relative positions as when the photos were collected. At this point, the left and right projected light sources form a single light path superimposed on a 3-D view of the ground surface. If proper stereo orientation is not achieved, parallax offset of common object points on the photos will result in separation of left and right image dots, which appear to float above the ground or rest beneath it relative to the stereo view of the ground surface. Only when the dots are superimposed and visually appear to sit precisely on the ground surface can 3-D coordinates be extracted from the model. Additional adjustment to the mechanical carriage is made to level the model relative to the tracing stand or geographic plane of the model.

Stereo models were originally scaled to ground coordinates by physically linking the photo carriage to a pantograph arm, which carried a pencil and was

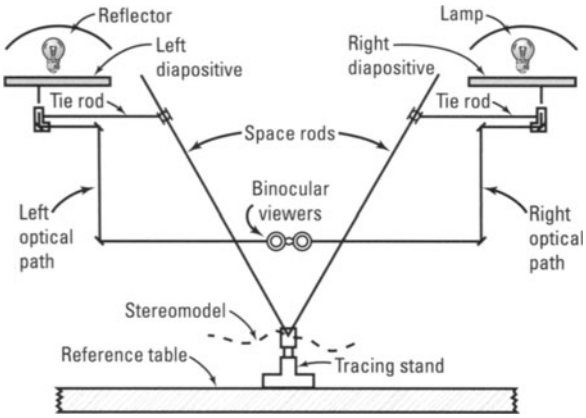

Figure 6.10. Sketch of a typical configuration of an analog stereoplotter, including the optical-viewing system, measuring and tracing system, and reference or tracing table (modified from Wolf and Dewitt, 2000).

used to translate motion of the instrument to projected lines drawn on base materials. Relative movements of the mechanical carriage were translated to the appropriate degree of motion of the pantograph arm by a series of gears in combinations that corresponded to the scale of the geographic base map. Most analog systems still in use today have been retrofit with digital encoders to translate the x, y, and z motions of the mechanical carriage into digital streams of coordinate triplets that are passed to digital-mapping applications. Because of the mechanical limitations of these systems, they are only suitable for work with aerial photographs collected with minimal camera-axis rotation. Although limited in the range of application, these instruments are extremely precise, have excellent optics, and, after interior, relative, and absolute orientations are complete, are easy for a geologist to operate. Additionally, stereo models can usually be oriented with no knowledge of the original camera beyond its focal length. This advantage makes these instruments particularly well suited to analysis of a large database of archived imagery that might lack accompanying camera-calibration reports.

6.4.2 Analytical stereoplotters

Analytical stereoplotters became readily available during the 1980s with the advent of low-cost microcomputers, digital encoders, and servo controllers. These stereoplotters are designed around an analytical solution to a photogrammetric orientation. The fundamental characteristics of these instruments are an ability to precisely drive to defined x and y coordinate positions on left and right image carriages, and to accurately measure photo coordinates on the rectified image pair. This is accomplished by controlling image-plate motions with high-precision servo motors linked to electronic operator controls for positioning the camera plates and the floating mark. Optical systems include high-power binocular viewing and variable light source controls, which help to maximize image measurement capabilities. Analytical stereoplotters remain the highest precision photogrammetric instruments available, often claiming precision tolerances within three microns on the film plane.

Analytical stereoplotters compute a mathematical model for the interior, relative, and absolute orientation of a stereo model and translate operator controls to photo-plate motions based on the orientation. This facilitates automated data collection, especially for digital elevation model (DEM) collection, by allowing automated grid positioning. Grid spacing is predetermined and the stereoplotter drives the floating mark to the proper x, y coordinate position on the photo. The operator uses the stereoviewing system to place the floating mark on the ground, fixing the z coordinate in space based on the photogrammetric-model orientation. The ability to drive the instrument also aids in data collection for features such as geologic contacts in mapping applications, by enabling the operator to edit vector line work while the instrument drives the floating mark to the node position indicated by the mapping software.

The calculation of the z coordinate in analytical systems and softcopy systems requires that two conditions be satisfied: (1) collinearity for a single photograph, and (2) coplanarity for a stereo pair. These conditions are mathematically represented by two non-linear equations, one for the x coordinate and one for the y coordinate, based on the parameters of the interior, relative, and exterior orientations. The equations can be transformed to a series of linear expressions that are solved simultaneously and iteratively to determine the 'best-fit' z coordinate for any x, y pair. This procedure is represented graphically in Figures 6.11 and 6.12. Collinearity requires that the exposure station, any object point, and associated photo image point must all lie along a straight line in 3-D space. In the example shown in Figure 6.11, L, a, and A all lie along a straight line. Coplanarity requires that two exposure stations of a stereo pair, object point, and the associated image points on the two photos must all lie in a common plane. In Figure 6.12, points L_1, L_2, a_1, a_2, and A all lie in the same plane, enabling

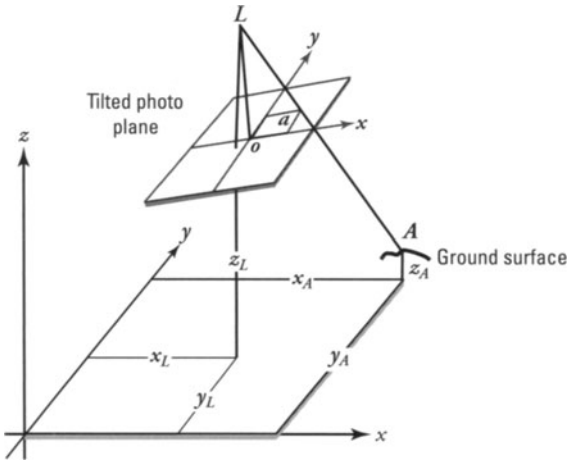

Figure 6.11. Illustration of the collinearity condition for any point *A* on the ground surface and its equivalent image point on an aerial photograph (modified from Wolf and Dewitt, 2000). See text for discussion.

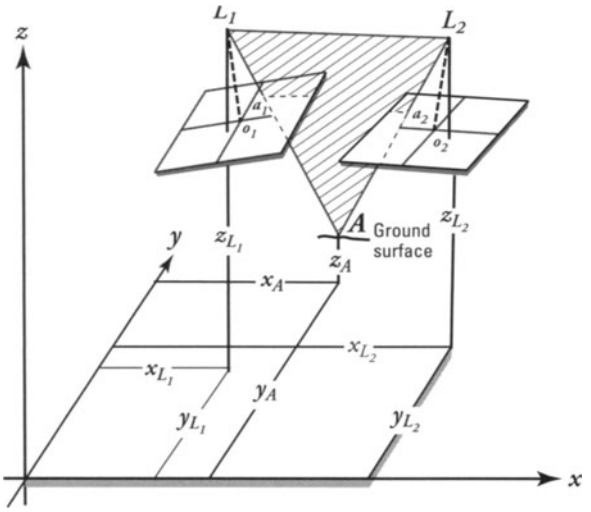

Figure 6.12. The condition of coplanarity for any point *A* on the ground and its equivalent image points a_1 and a_2 in a stereo model (modified from Wolf and Dewitt, 2000). See text for discussion.

iterative determination of the z coordinate for any object point in the stereo model. These calculations are performed in real time as the operator drives the analytical stereoplotter and positions the floating mark on the ground surface in the model.

6.4.3 Softcopy stereoplotters

Softcopy photogrammetric systems are essentially analytical stereoplotters that utilize digital images and software for translation of images, instead of mechanical control of image movement. Softcopy systems evolved from analytical stereoplotters as high-precision film scanners and high-speed computing platforms were developed, enabling creation and manipulation of high-resolution digital imagery in real time (American Society of Photogrammetry and Remote Sensing, 1996a, 1998; Graham *et al.*, 1997; Gwinner *et al.*, 2000). Modern photogrammetric scanners are capable of distortion-free, 7-micron scans resulting in image files in excess of a gigabyte each, with sufficient resolution to rival measurement capability of many analytical stereoplotters, despite a somewhat degraded viewing system. Although softcopy systems offer all of the advantages of conventional analytical stereoplotters, with the possible exception of the viewing system, its capacity for automated measurement based on image matching algorithms has catapulted this technology to the forefront of modern photogrammetry. The simplification of hardware requirements for softcopy systems has been accompanied by a dramatic increase in the complexity of associated software, leading to fierce market competition for what is, in effect, a software tool with minimal hardware requirements relative to those for analog and analytical stereoplotters.

6.4.4 Display systems

The basic hardware requirements for a softcopy system include a stereo-viewing system, high-speed central processing unit (CPU), and several hundred gigabytes of data-storage capacity. The two most common types of viewing systems both employ large cathode ray tube (CRT) monitors with 120-MHz screen refresh rates alternating views of the left and right photo image of a stereo model pair 120 times per second. The most comfortable viewing system employs an active polarizing filter fitted to the CRT screen and a lightweight pair of passive polarized glasses for the operator to wear. The active polarizing filter alternates the polarizing orientation at the same refresh rate employed by the CRT for displaying left and right images of the model pair. The glasses have left and right lenses with opposite polarizations, corresponding to those used by the active screen. When the computer displays the left image, the active polarizing screen blocks the view from the right eye. This alternates with display of the right image, blocked to view by the left eye, at a rate of 120 times per second; too high to be perceived by the human brain. The alternating projection of the overlapping images provides visualization of the area of overlap in stereo. An alternative method employs the same alternating display of left and right images on the CRT, but uses an infrared

signal keyed to the screen refresh rate that controls active polarizing lenses in headgear that alternates blocking the left and right images from view.

In both systems, the images are either panned relative to a fixed floating mark in the center of the screen, or the floating mark is allowed to track sequentially across the fixed stereo model. The floating mark, the ground surface, and any point or line data collected are viewed in 3-D, enabling immediate evaluation of adherence to the ground surface. Zooming is accomplished by sequentially displaying smaller regions of the digital stereo model, while increasing the displayed resolution to maintain a fixed image dimension. This is implemented in real time by maintaining multiple copies, typically up to seven, of the same image at successively higher resolutions. Maintaining multiple image copies not only aids zoom and pan operations, but also provides a means to apply image matching algorithms during the orientation procedure.

6.4.5 Computer-assisted orientation

Orientation of softcopy imagery involves the same steps required when using analog or analytical systems, with the advantage of additional image-matching capabilities inherent in all digital photogrammetric systems. Interior and relative orientations are greatly assisted by utilizing *image pyramids*, or linked image layers representing successively higher resolution versions of a given image area for each scanned photograph. Having multiple copies of the same image at different resolutions enables rapid identification of fiducial marks for interior orientations and of *pass points* (i.e., points common in three successive images used in relative orientations).

For orientations, fiducial marks are recognized automatically by matching image pixel patterns to templates identifying styles of marks utilized by different camera manufacturers. Alternatively, unknown fiducial patterns can be 'learned' by most systems and recognized in subsequent photographs. Fiducial marks are measured using pattern recognition for successively higher resolution scans and by digitally constraining the floating point to occupy the center of the marks. After fiducial marks are measured, the principal point of the digital photos is calculated by resecting lines connecting individual fiducial marks.

Combined with knowledge of the focal length and lens distortion parameters of the interior orientation, a relative orientation can be performed by identifying pass points common to both photos of a stereo pair or three photos in multi-model strips. Pass points are identified by using pattern recognition and image-matching algorithms that initially search low-resolution photos for coarse object patterns common to left and right images of the stereo model. Then the algorithms successively zoom in to higher resolution images, refining the pattern search to occupy x and y coordinates of common pixels. Analog and analytical stereoplotters typically require a minimum of three manually determined points to constrain a relative orientation. Usually, more points are collected to provide sufficient redundancy in an analytical solution; this can be a tedious manual process. Softcopy stereoplotters typically calculate many (up to hundreds) pass points for use in the relative orientations, thereby minimizing the impact of errors associated with any given point. Automatically generated pass points with high residual errors associated with the orientation can be removed from the solution, and the relative orientation can then be recalculated.

Despite the automation inherent in interior and relative orientations (Hannah, 1989; Kersten and Haering, 1997), absolute orientation requires operator input to visually identify ground control with known positional coordinates in both the left and right photos. In conventional photogrammetry, these are indicated in the photos by GPS or survey control points marked with white or black plastic panels (photo targets). After the x and y coordinates of these control points have been measured monoscopically in the left and right images, an analytical solution to the exterior orientation is performed. When the errors associated with control point measurements have been determined, control points can be re-measured, added, or deleted to optimize the best-fit solution. Upon completion of the exterior orientation, stereo models are viewed in three dimensions, point and line data are collected and viewed in three dimensions, and derivative products such as digital elevation models and orthophotos are produced.

6.4.6 Digital elevation models

Digital elevation models (DEMs) are mathematical representations of topography based on x, y, z coordinate sampling of the ground surface at regular grid intervals. These datasets can be used to produce topographic maps or detailed mathematical models of the ground surface. They

provide critical quantitative data to volcanologists monitoring geomorphic change at active volcanoes or conducting predictive modeling of volcanic hazards such as dome growth (Robertson *et al.*, 2000) or lahar runout (Iverson *et al.*, 1998).

DEMs can be collected on analytical stereoplotters by forcing the instrument to occupy x and y coordinate positions in a stereo model as the operator places the floating mark on the ground to determine the z position at each grid node. This produces a very accurate DEM, but it is time consuming and leads to operator fatigue for large grids with many nodal points (perhaps thousands). Softcopy stereoplotters utilize the same pattern-recognition and image-matching algorithms employed in the determination of pass points to calculate x, y, and z coordinates for nodal points on grids, with spacing determined by the operator. This requires solving the collinearity and coplanarity equations for every node on the grid. The process is automatic with most systems and requires no input from the operator during the calculation of the model.

An accurate representation of the ground surface, especially in areas of high relief, usually requires additional information for calculation of accurate DEMs. *Breaklines*, or x, y, z coordinate strings representing the tops of ridges or the bottoms of valleys, and individual points representing peaks or objects of interest, are collected manually and provided as input to the surface-generating (DEM or triangulated irregular network, TIN) software. During the creation of the DEM or TIN, the manually collected points force the grid surface to follow these important inflections in the topography. The creation of a high-quality DEM typically is an iterative process in which successively higher resolution models are produced by successively decreasing the grid size of each model iteration. This forces the DEM calculations to conform to points generated in the previous, lower resolution model. Performing the calculations in this fashion minimizes the amount of editing required, because a percentage of points in any given calculation will be incorrectly placed either above or below the ground surface as a result of incorrect image correlation.

6.4.7 Orthophotos

Digital orthophotos are photogrammetrically rectified photo images derived from aerial photographs and a DEM. Orthophotos have the distinct advantages for field applications of having both the image qualities of aerial photographs and the cartographic registration necessary for mapping and measurement purposes. The critical requirements for the creation of digital orthophotos are a high-quality DEM and digital aerial photographs having known exterior-orientation parameters. The process is based on the application of the collinearity condition for any point of the DEM to relate x and y position coordinates to a given pixel, or series of pixels, in the associated photograph. Repetitive application of the collinearity condition for every point of the DEM results in population of the x and y matrix with corresponding image pixels, resulting in the orthophoto image (Hohle, 1996).

6.4.8 Satellite imagery

The rapidly increasing availability of commercial satellite imagery, especially in the visible and radar portions of the electromagnetic spectrum (Theodossious and Dowman, 1990; Weston, 1990), has generated considerable interest in the potential for photogrammetric exploitation of this data for three reasons. First, commercial optical sensors have an image resolution of ~ 1 m and regional radar imagery is now available with better than 50 m resolution. Such resolutions are suitable for many mapping applications and the satellite images have the advantage of a significantly larger image footprint for any given scene. A second reason is that satellites provide predictable and repeatable image coverage, which makes them ideal platforms for monitoring applications. Radar waves can penetrate clouds and, to a degree, airborne dust, so satellite radar imaging holds promise for 'seeing' through clouds and ash during an eruption, when other imaging systems are less effective. Third, softcopy stereoplotters are readily adapted to accommodate digital imagery of all types, which makes them a particularly flexible tool.

Most imaging satellites use linear-array sensors, which acquire images along scan lines that are perpendicular to the path of the satellite. Because satellites are highly stable platforms with predictable flight paths and imaging geometry, stereo images suitable for photogrammetric rectification are routinely collected by such systems. The details of the scanning geometries associated with commercial satellites are routinely made available to photogrammetry software vendors, with hopes that they will incorporate scanning imagery into the mainstream of softcopy systems. Photogrammetric applications of satellite imagery are beyond the scope of this chapter, but the interested reader is

referred to Weston (1990) and Theodossious and Dowman (1990) for a description of photogrammetric rectification using commercial SPOT satellite imagery. Utilization of higher resolution IKONOS and QuickBird imagery and RADARSAT datasets is becoming more common, and several commercial software vendors already offer orientation packages with satellite-specific geometric solutions for interior, relative, and absolute orientations.

6.5 AEROTRIANGULATION

Aerotriangulation is the general term for the method used to bridge control between photos within a strip of stereo models or a block of multi-model strips. Exterior orientation of single stereo models requires a minimum of five control points, two of which have x, y coordinates and three of which have elevation or z-coordinate control. As discussed above, these can be combined such that two horizontal control points with vertical control serve as two of the three z-control points, reducing the total number of points required to three. These photogrammetric solutions for single-model stereo pairs are relatively easy to perform on analytical or softcopy stereoplotters, but they require a high density of control points for each model solution. For small projects, control can be passed along the strip from model to model, but this introduces photogrammetric error that tends to increase the farther the solution is carried down the strip. The only way to avoid this problem is to perform a strip or block adjustment based on aerotriangulation that incorporates control from geodetic markers, large enough to be visible in the photos, strategically placed at ground survey points in the study area. This is usually accomplished with panels made of cloth, plastic, wood, or similar material positioned in a symmetrical pattern centered on bench marks or other survey points prior to the photo flight.

Geologic projects designed around mapping or monitoring applications based on aerial or terrestrial photography comprise multiple models or multiple strips of photos and require complex analytical orientation solutions. Fortunately, the mathematical derivations of these solutions, though complex, are well documented (Wolf and DeWitt, 2000, and references therein) and are available as part of orientation software packages on most analytical photogrammetric systems. There are numerous aerotriangulation schemes for orienting strips or blocks of photographs. Most are optimized for particular types of images or numbers of photos included in the orientation. For our purposes, these schemes can be discussed in generic terms by describing the mechanical steps an operator performs when doing an aerotriangulation adjustment (sometimes referred to as a 'bundle adjustment').

The general procedure involves the same steps required to perform any standard photogrammetric orientation, including: (1) interior and relative orientation of individual stereo models; (2) connection of adjacent models to form continuous strips or multiple strips; and (3) absolute orientation, tying the adjusted model to ground-control coordinates. Basically, aerotriangulation uses condition equations that represent the unknown elements of absolute orientation of each photo in the strip or block in terms of camera parameters, internal photo coordinates, and external ground coordinates. These relationships are expressed as a series of over-determined, non-linear expressions with many unknowns. The expressions are transformed by Taylor's theorem[3] into a series of linear equations that can be solved simultaneously once initial boundary conditions are established. In the same sense that orientation of stereo models on an analog stereoplotter involves iterative reduction of error about any geometric variable on the instrument, aerotriangulation is a numerical solution that minimizes photogrammetric error across the entire strip or block of stereo models. The most common form of equations employed for this purpose describe the condition of collinearity which, as we have seen, is essential to analytical and softcopy photogrammetric orientation of single models.

The most immediate benefits of aerotriangulation in geodetic studies at volcanoes are: (1) ground control can be minimized across the project area, (2) the aerotriangulated solution provides independent evaluation of the geodetic ground control, and (3) the final solution provides for full-field 3-D geodetic control.

A diagrammatic representation of interior pass points and exterior ground control for a typical strip and block of photos is depicted in Figure 6.13. The total number of ground control points necessary for orientation of the entire strip or

[3] In calculus, Taylor's theorem, named after the mathematician Brook Taylor, who stated it in 1712, gives the approximation of a differentiable function near a point by a polynomial whose coefficients depend only on the derivatives of the function at that point. The most basic example is the approximation of the exponential function near $x = 0$:
$e^x \approx 1 + x + (x^2/2!) + (x^3/3!) + \cdots (x^N/N!)$.

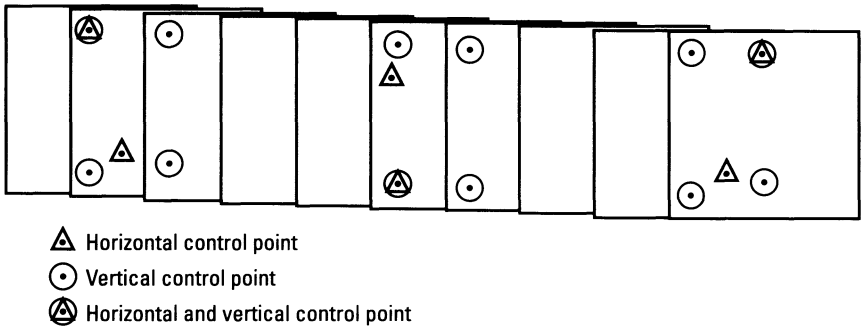

Figure 6.13. Control point configuration for aerotriangulation of a single-strip project consisting of 9 stereo models and 10 photos (from Wolf and Dewitt, 2000). The diagram represents an ideal situation in which control is available in the center of the strip; however, the aerotriangulation can also be performed with control only on both ends. See text for details.

block of photographs is reduced by nearly an order of magnitude relative to that required for the corresponding series of individual stereo models. This is only possible because of the strength of the relative orientation, which is based on the availability of photo identifiable pass points common to adjacent images. The positions of pass points can be measured independently on each photo in analytical stereoplotters, or they can be determined automatically using image-matching algorithms in digital softcopy systems. The great advantage of softcopy systems in this regard is that many pass point measurements can be made in a short period of time, increasing redundancy in the simultaneous equations that are solved for the aerotriangulation, and consequently reducing the error associated with the final solution. Upon convergence, an aerotriangulated solution provides an indication of residual errors associated with any given control point in the exterior orientation, and also a mean residual error associated with the entire orientation. These control point errors can be compared with the errors associated with the original geodetic control point measurements. Large deviations that exceed the residual errors or high residual errors associated with the aerotriangulated solutions indicate a photogrammetric bust in the control point data, which can be attributed to errors in the original control point measurements. In some circumstances, weighting control points relative to the first-order errors associated with individual control point measurements can reduce the mean residual error for the project as a whole. Control points with the lowest first-order measurement errors are given preference over less well-determined ground control in the final solution. Typically, this is not a problem with modern GPS ground control, but it can be an issue when using conventional survey control. Upon completion of an aerotriangulated solution, every point within any stereo model encompassed by the solution has an associated error equal to the mean residual error of the solution.

6.6 TERRESTRIAL PHOTOGRAMMETRY

Terrestrial photogrammetry refers to photogrammetric analysis of photos taken with cameras at ground locations. Historically, a distinction has been drawn between photographs taken from less than approximately 300 m and those taken at greater distances. The former is typically referred to as close-range photogrammetry. Applications in volcanology encompass a wide range of camera-to-object distances, and commonly employ low-altitude aerial platforms such as helicopters or light aircraft in addition to camera stations on the ground. As the distinction is photogrammetrically irrelevant, we have opted to include all non-conventional aerial photography in this discussion under the heading terrestrial photogrammetry.

Two classes of cameras are used in terrestrial photogrammetry. Metric cameras are those designed specifically for photogrammetric use; non-metric cameras include all others. This distinction is made regardless of the type of camera (i.e., a film-based or CCD digital imaging camera). Metric cameras have factory calibrated lenses, reliable construction, vacuum backs for film stabilization, and permanent fiducial marks in the film plane for accurate and repeatable determination of the principal point. Geologists most often use less sophisticated non-metric cameras, typically either (1) 35-mm or medium-format film cameras, or (2) point-and-shoot or single-lens reflex (SLR) digital cameras, which serve double duty as standard field cameras. Only one 35 mm and one medium-format film camera in this category have vacuum backs for film stabilization, but nearly all can be fitted with high-quality, single-focal length lenses suitable for photogrammetric work. Digital

cameras, by design, do not require vacuum backs. High-quality, interchangeable lenses designed specifically for use with digital SLRs are widely available, and, in some cases, lenses designed for use with film cameras can be used with digital camera bodies.[4] In either case, the lens should be calibrated for photogrammetric applications.

Lens calibration is essential when using non-metric cameras in photogrammetric applications. Calibrating lenses provides four pieces of information critical to performing interior orientations with terrestrial photographs. The first two are determined by photographing an object of known dimensions, usually a 3-D grid, from multiple angles and inverting the interior orientation solution to solve for the unknown lens parameters. Determination of the second two parameters is more subjective and requires knowledge of both the lens and camera body.

A camera's calibrated focal length represents the distance from the *nodal point* of the lens to the principal point of the photograph. For aerial cameras, this is equivalent to the optical focal length of the lens, but the same is not necessarily true for hand-held, non-metric cameras. Unlike metric cameras, non-metric cameras utilize standard photographic lenses, which commonly produce noticeable *radial lens distortion*. This is observed in standard photographs when horizontal or vertical objects near the outer edges of the photograph appear curved, either inward or outward. This distortion tends to be symmetric and radially distributed outward from the principal point of the lens (Figure 6.14). Modern, high-quality, wide-angle to normal focal length photographic lenses with low to moderate radial distortion are easily calibrated and lend themselves well to terrestrial photogrammetry. These can be either conventional film camera lenses or newer versions designed specially for use with digital SLRs.

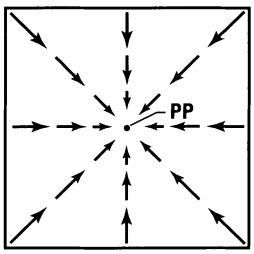

Figure 6.14. Radial distortion pattern characteristic of small- and medium-format camera lenses most commonly used in terrestrial photogrammetry. Arrow tails represent positions of points in object space; heads represent corresponding, distorted positions in image space. Object points nearer to the edges and corners of the lens' field of view are displaced to a greater degree in image space than those nearer to the principal point (PP).

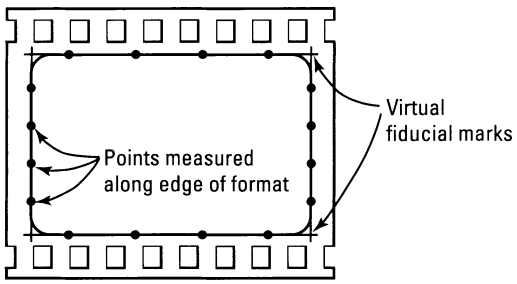

Figure 6.15. Asymmetric or non-square corners on small- and medium-format film positives require extrapolation of photo edges to establish fiducial marks (from Wolf and Dewitt, 2000).

Non-metric, small- and medium-format cameras have no fiducial marks visible in the image plane. *Fiducial marks* provide the x and y coordinates of the edges or corners of the film image. These marks are necessary for calculation of the principal point of the image, usually the intersection of obliquely opposing corner marks, and for establishing the position of the images themselves. The corners of image frames can be used, but they are rarely square (Figure 6.15). In most cases, the frame edges forming a given corner can be extrapolated to the point where they intersect, and this point can be used in lieu of corner fiducial marks. It is important to note that the geometry of the image corner is directly related to the film mask of the camera body in use. Hence, calibration usually refers to lens and camera combinations in non-metric applications.

A critical uncertainty in terrestrial photogrammetry using non-metric cameras is the effect of film-plane instability. Interior orientation of small- and medium-format images assumes the film plane is flat across the entire field of view. Cameras with vacuum

[4] When a lens designed for use with a 35-mm film camera is used with a digital SLR, the focal length of the lens must be multiplied by a factor that depends on the size of the camera's image sensor. If the image sensor is full-frame (i.e., the same size as 35-mm film), then the multiplier is 1. However, only a few digital SLRs use full-frame image sensors. Most are smaller and, consequently, the multiplier is greater than 1. For example, a conventional 55-mm lens, when used with a digital SLR with a typical focal-length multiplier of 1.6, has an effective focal length of ~88 mm – and a correspondingly narrower field of view. Two salient points to consider when choosing a camera lens combination for photogrammetric applications are: (1) the imaging system's field-of-view and resolution should be consistent with other mission parameters and requirements (e.g., flight altitude, desired DEM accuracy); and (2) for best results, the lens should exhibit minimal radial distortion and must be calibrated.

film backs actuated at the moment of shutter release can approach this condition and reduce this uncertainty essentially to zero. Alternatively, digital CCD-based cameras with a fixed geometry can be used, thereby eliminating this uncertainty altogether. Non-metric film cameras, on the other hand, suffer from variations in film flatness by up to an order of magnitude across the film plane, typically ranging from zero to ten microns. Such deviations are comparable to the measurement capability of many analytical instruments, and therefore they introduce unknown errors to a photogrammetric solution. However, these errors might be insignificant for many geologic applications.

Collecting suitable terrestrial imagery can be as simple as photographing handheld stereo pairs from the ground or air along linear traverses, or as complex as rigorously establishing GPS control for each camera position and monitoring three camera-axis rotations for each photograph (Dueholm, 1992; Dueholm and Pedersen, 1992; American Society of Photogrammetry and Remote Sensing, 1996b). The more information that is available for camera position and orientation, the less ground control is necessary for exterior photogrammetric orientation. Nearly all ground control established for terrestrial applications in volcanology comes from one or more of the following: (1) GPS ground control established at visibly identifiable control points within the terrestrial imagery; (2) visually identifiable control point targets whose positions can be determined by conventional survey techniques; or (3) transferred coordinate data from photogrammetrically rectified aerial photographs. External GPS control or survey control is minimal or not readily available in many volcanically active regions; in such cases, absolute orientation is limited to control transferred from existing aerial photography. For many applications, this provides adequate geodetic control to establish a ground-coordinate datum from which relative geomorphic changes, such as those associated with dome growth, can be rigorously modeled based on relative, as opposed to absolute, position changes.

Terrestrial photogrammetry associated with geodetic monitoring is typified by single strips of overlapping photographs obtained at an oblique angle to the horizontal datum, either looking down into volcanic craters and steep canyons, or up at crater walls and mountain fronts. These situations are characterized by large scale changes across the photograph or strips of photographs, which can result in loss of stereo coverage in parts of individual stereo pairs or across the strip. This problem usually stems from unanticipated variation in the geometry of the camera orientation relative to the ground, or failure to accommodate sharp changes in relief with corresponding changes in base length of the photography. Loss of stereo coverage can be mitigated by varying the photographic interval across the length of the photo mission, in such a way as to accommodate changes in topographic relief. Inadvertent variation in camera orientation can often be avoided by maintaining a distinct line-of-sight relative to the horizon in the camera's viewfinder, and by tracking the progress of a visually distinct image object through the viewfinder. Tripping the shutter after the object of interest moves 40% of the way across the field of view yields 60% stereo coverage in the resultant image. In some cases, multiple strips might be flown at different scales to ensure proper stereo coverage.

The United States Geological Survey (USGS) David A. Johnston Cascades Volcano Observatory (CVO) is using both conventional 9×9 inch vertical aerial photographs and small-format oblique stereo photographs to track the dome-building eruption that began at Mount St. Helens in September–October 2004 (Dzurisin *et al.*, 2005). The oblique photos are useful for extending stereo coverage into areas that are obscured in the vertical photos by unavoidable clouds, deep shadows, or the eruption plume.

6.7 APPLICATION TO MOUNT ST. HELENS

The catastrophic eruption of Mount St. Helens on 18 May 1980, involved or initiated geologic processes that produced geomorphic changes amenable to both short- and long-term photogrammetric monitoring. Post-18 May activity included smaller explosive eruptions during summer 1980, and episodic lava dome growth through October 1986 (Swanson and Holcomb, 1990). Contemporaneously, frequent rock avalanches from the steep and unstable crater walls resulted in their rapid retreat and in the formation of large talus cones (Mills, 1992). Within a few years, snow, ice, and rockfall debris accumulating on the crater floor formed a new glacier, the youngest in the Cascade Range (Schilling *et al.*, 2002, 2004). Although some aspects of the activity, particularly dome growth at Mount St. Helens and more recently at active vol-

canoes elsewhere (Jordan and Kieffer, 1981; Zlotnicki and others, 1990; Achilli *et al.*, 1998; Baldi *et al.*, 2000), have been analyzed quantitatively using aerial photogrammetry, few active volcanoes are as well characterized through archival aerial photographs as Mount St. Helens. This archival database, spanning two decades and counting, enables quantitative characterization and reconstruction of all aspects of geomorphic change and re-glaciation at the volcano.

Determination of volumetric changes associated with geomorphic change at Mount St. Helens requires systematic retrospective photogrammetric aerotriangulation of aerial photography of the volcano's crater and flanks, followed by DEM extraction from the stereo photography, and determination of volumetric change as a function of time based on DEM grid calculations. The ability to make these determinations in real time using softcopy photogrammetric systems has largely gone unrealized, but it will likely influence future monitoring efforts at Mount St. Helens and elsewhere. For example, Robertson *et al.* (2000) used photogrammetric analysis to develop predictive models of dome growth during the eruption of the Soufrière Hills Volcano, Montserrat, that began in 1995. In addition, geologic mapping of the largely inaccessible Mount St. Helens crater walls based on terrestrial photogrammetry affords geologists a rare opportunity to reconstruct the 3-D geologic record of a young Cascades stratovolcano (Singer *et al.*, 1997; Dungan *et al.*, 2001).

During the years following the 1980 eruption of Mount St. Helens, aerial photographs were used to construct large-scale contour maps of the growing dome (Swanson and Holcomb, 1990), and to estimate the volume of snow and rock accumulation within the crater moat (Mills, 1992; Mills and Keating, 1992). Mills (1992) described the crater walls as one of the most rapidly eroding places on Earth. Frequent and nearly ubiquitous rockfalls spalled off the steep, unstable crater walls and were, in part, incorporated in the growing lava dome. In 2005, rockfalls were still nearly continuous from the crater walls in summer and fall. In winter and spring, the walls are stabilized by moisture trapped mainly as snow and ice – a condition that has prevailed since the crater formed in 1980. As the moat continued to fill with rock, snow, and ice throughout the 1990s, crevasses began to form in the crater fill, indicating the presence of a new glacier. As the glacier grew, so did the concerns of public officials, planners, and emergency managers, who were aware that any new eruptive activity posed a threat of hazardous lahars or debris flows in the North Fork Toutle River valley. Photogrammetry provided an affordable means to address these concerns and to estimate the volume of talus, snow, and ice in the crater.

Determining the change in volume of geomorphic features in the crater is based in part on a high-resolution, high-accuracy DEM created from 1 : 12,000 scale aerial photographs flown in September 2000. Photogrammetric ground control was based on a network of GPS control targets in the crater and on the outer flanks of the volcano. Precise aerotriangulation of four strips of aerial photographs enabled autocorrelation of hundreds of thousands of x, y, z coordinates and extraction of a TIN surface using commercial softcopy photogrammetric software. The resulting topographic model can be used to calculate volume changes by differencing with models for earlier epochs, and it provides an accurate and well-characterized baseline for analysis of future geomorphic changes.

Roving GPS receivers were used to occupy control points in the study area, which were paneled with standard aerial photography targets. GPS observations were collected for approximately 1 hour at each point and differentially corrected using data from the continuous GPS station JRO1 at the Johnston Ridge Observatory, 9 km north of the crater. Accuracy associated with the resulting aerotriangulation for the entire volcano is on the order of a few centimeters, based on both GPS and photogrammetric uncertainties. High precision resulting from the internal orientation enabled highly accurate placement of TIN surface points and breaklines. The detailed TIN surface for the crater derived from year 2000 aerial photographs was used in combination with the elevation of TIN points and interpolated elevations from TIN facets to create a DEM. The configuration of control points and examples of overlapping aerial photographs are shown in Figure 6.16.

The high degree of accuracy and precision associated with the year 2000 model can be applied to archival models while collecting precise TIN surfaces (i.e., control points visually identified in the 2000 model that fall outside of the region of change can be identified in the archival photography and assigned x, y, z coordinate positions determined from the 2000 aerotriangulation). These new control points in the archival photography are treated as standard ground control points in the subsequent aerotriangulation of the archival strips of aerial photography. In this manner any number of

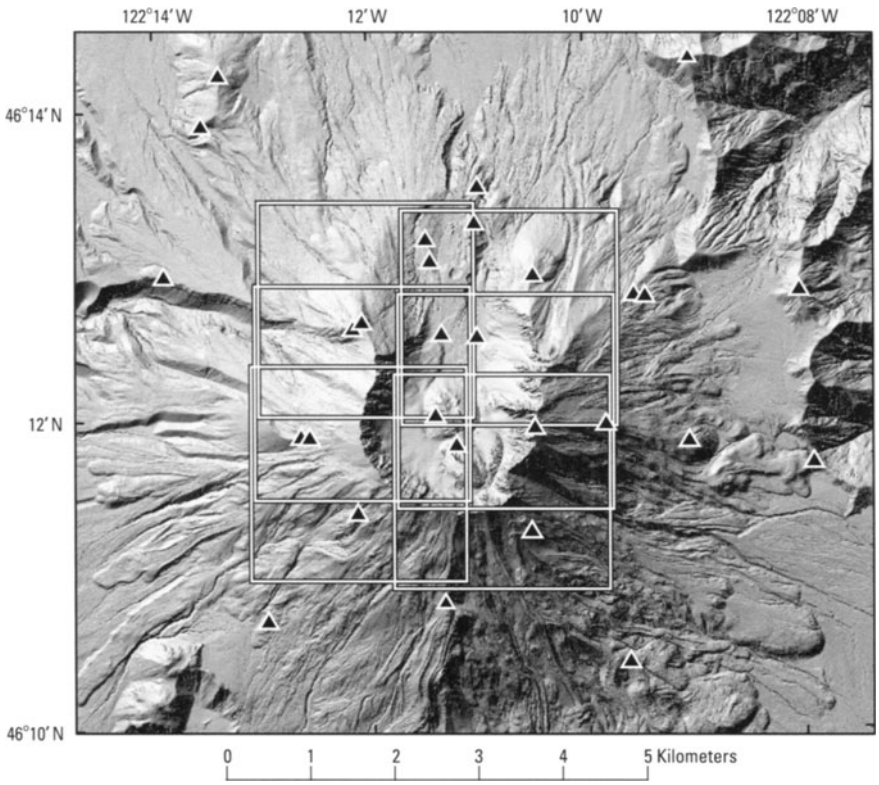

Figure 6.16. Example of aerial photo coverage used to produce a series of DEMs for Mount St. Helens from 1980 to 2005, including the September 2000 DEM discussed in the text. White squares represent the extent of single aerial photographs, overlapping about 60% along north–south flight lines with about 30% sidelap between adjacent flight lines. Black triangles represent control points included in photogrammetric analyses. Shaded relief depiction is based on a November 2003 DEM from lidar and an April 2005 DEM from photogrammetery. Graphic created by Sarah K. Thompson and Steve P. Schilling, USGS.

archival datasets can be used for quantitative extraction of geodetic data without having had the benefit of original ground control. The same approach can be used to visually transfer control into future sets of aerial photographs, even if the original control points are no longer visible.

Even though we have not yet constructed TIN surfaces from previous years of crater aerial photographs, as a preliminary estimate we generated DEMs from 1 : 24,000 scale digital contours constructed from aerial photographs taken in 1980 (published USGS topographic map) and 1989 (unpublished map data). The vertical accuracy of the DEMs created from contours is derived from the accuracy of the contours. National Map Accuracy Standards specify that the vertical accuracy for contours is one-half of a contour interval (i.e., 20 feet or about 6 meters in this case). The DEM elevation values are taken from the contours or interpolated between contours using an algorithm with eight-way, inverse-distance weighting. The algorithm uses, with appropriate weighting, the distances from each element in the DEM to the first contour encountered in each of the four cardinal and four intermediate directions (N, NE, E, SE, S...) to compute an elevation for each element. Closer contours are assigned greater weight. The Mount St. Helens DEMs span two decades (vintage October 1980, September 1989, and October 2000) and share a common projection (Universal Transverse Mercator, zone 10), horizontal datum (NAD27), geographic location, and 10-m cell size. Each of the three surfaces is shown in gray shaded relief and colored perspective view in Figure 6.17. In the shaded-relief view, white lines sketched from the 1989 DEM mark the crater rim and outline the 1980–1986 lava dome; an intervening line separates areas of erosion from areas of deposition as determined by subtracting the 1980 DEM from the 2000 DEM.

We calculated volume changes by subtracting one DEM surface from a second one, after ensuring proper alignment of grid cells from one surface to the next, using ArcINFO geographic information system (GIS) software. The absolute values of all resulting negative cells (erosion or subsidence) and positive cells (deposition or uplift) were summed separately and multiplied by the area of a single cell ($100\,m^2$). Following a similar methodology established by Mills (1992), we took the total volume summed from positive values and subtracted the volume of the 1980–1986 lava dome. Then we

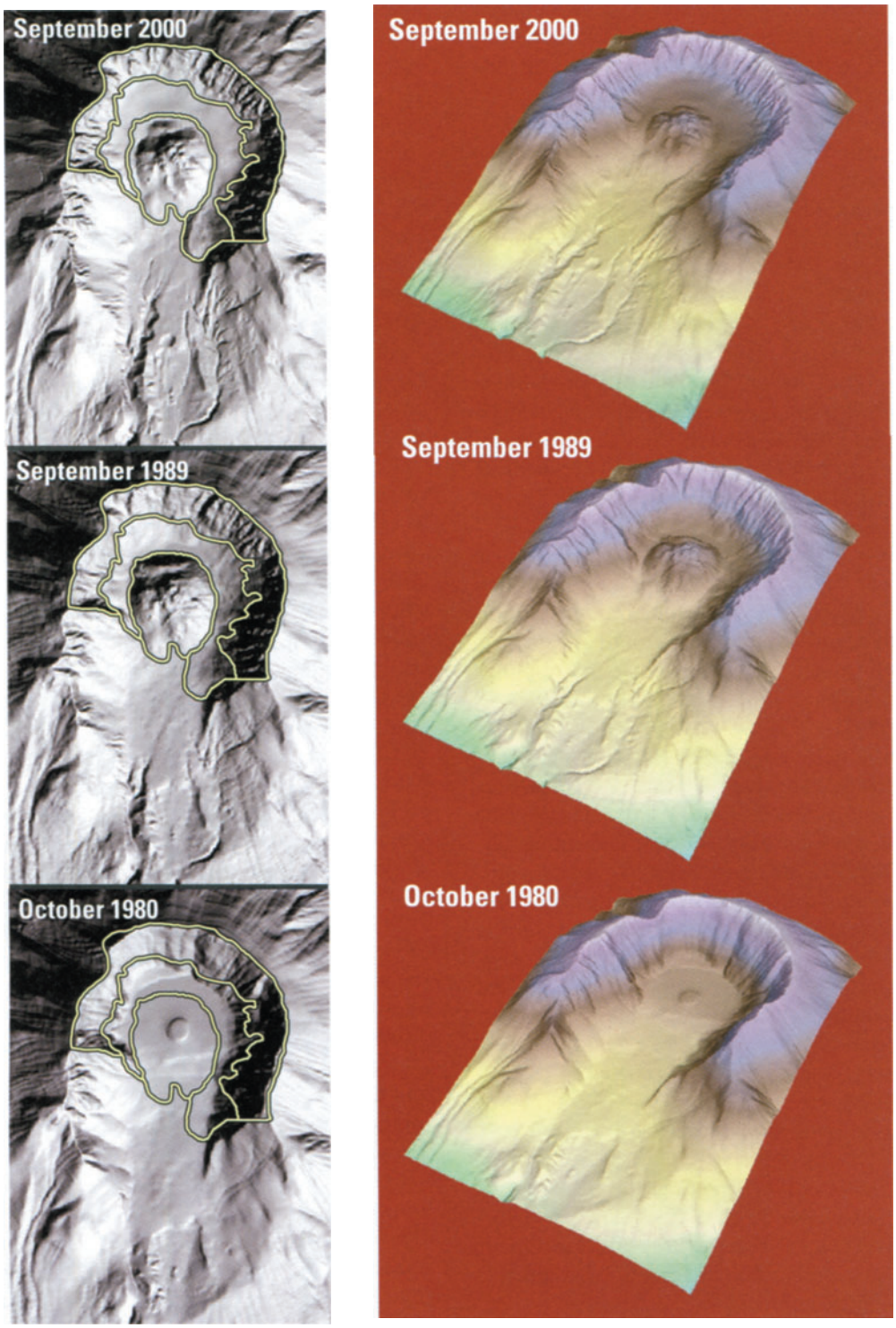

Figure 6.17. Shaded relief and perspective color contoured depictions (left and right, respectively) of three DEMs, showing surface morphology for the crater and upper flanks of Mount St. Helens for October 1980, September 1989, and September 2000. North is toward the bottom in the shaded relief images, and toward the bottom-left in the color contoured images. Yellow lines in the shaded relief images were sketched from the 1989 DEM; they mark the extent of the crater rim, the dome, and the intervening boundary between areas of erosion and deposition. Note progressive development of erosional channels on crater floor north of lava dome. The lava dome grew episodically from 1980 to 1986. Thereafter, the base of the dome was buried progressively by a combination of rockfall debris from the crater walls, annual snow, and perennial ice that together form the newest glacier in the Cascade Range (Schilling *et al.*, 2002, 2004).

subtracted the volume of rock eroded from the crater walls, assuming a closed system. The remaining volume is an estimate of the volume of snow and ice in the crater.

Dome growth at Mount St. Helens began in June 1980 and ceased in October 1986.[5] Aerial photographs were collected frequently during this six-year time period for purposes of visual monitoring, and some were used to construct detailed contour maps of areas within the crater (Swanson and Holcomb, 1990). To estimate the volume of the 1980–1986 dome, we subtracted the 1980 DEM from the 1989 DEM. Our result, 0.09 km^3, differs slightly from the 0.08 km^3 estimate of Swanson and Holcomb (1990), but it agrees well with the calculations of Mills (1992), who suggested the difference is due to Swanson and Holcomb's (1990) exclusion of crater wall debris that was incorporated into the dome as it grew.

The results of our calculations are depicted in Figure 6.18. The three images on the left (Figure 6.18(A)–(C)) show the magnitude and location of both negative values (erosion or subsidence) and positive values (deposition or uplift) obtained by differencing the DEMs for 2000 and 1980 (A), 2000 and 1989 (B), and 1989 and 1980 (C). The three images on the right (Figure 6.18(D)–(F)) show perspective views from northeast of the same surfaces as in (A)–(C), plus isopach surfaces of the net elevation changes for the same three intervals (floating surfaces). Each row in the figure shows three portrayals of the differences created by subtracting DEM surfaces of different vintages. For example, images in the top row show the results of subtracting the 1980 DEM from the 2000 DEM draped over a shaded relief image of the 2000 DEM ((A) and (D)), and also draped over an isopach surface of the net elevation changes during that interval ((D), floating). Similarly, the middle two images ((B) and (E)) show the result of subtracting the 1989 DEM from the 2000 DEM, and the bottom two images ((C) and (F)) show the results of subtracting the 1980 DEM from the 1989 DEM. Each of the images is color-coded: warm colors (red, yellow) for erosion or subsidence and cooler colors (green, blue, purple) for deposition or uplift.

From 1980 to 1989, the primary geomorphic changes within the crater were (Figure 6.18(C) and (F)): (1) growth of the lava dome from 1980 to 1986; (2) erosion of the steep crater walls by mass wasting; and (3) accumulation of talus, snow, and ice in the moat on the west, south, and east sides of the dome. During the ensuing decade (Figure 6.18(B) and (E)), the dome subsided slightly, probably as a result of cooling and compaction, while material continued to be shed from the crater walls and to accumulate in the moat. By 2000, the deepest fill in the moat was over 240 m thick between the south crater wall and the 1980–1986 dome (Figure 6.18(A) and (D)), and the total volume of snow and ice stored within the crater was approximately 80×10^6 m^3 (0.08 km^3) (Schilling *et al.*, 2002, 2004).

In addition to creating sequential DEMs that capture volumetric changes in the crater through time, we have used terrestrial photogrammetry to support detailed 3-D geologic mapping of the crater walls. The resulting maps document multiple eruptive and erosion cycles during the last millennium at Mount St. Helens. For the latter application, visually identifiable control, based on the year 2000 aerotriangulated model, was used to establish control in oblique aerial strips of stereo photographs collected from a helicopter flying north–south and east–west flight lines in the crater. The general configuration of the data collection for this terrestrial photogrammetric study is depicted in Figure 6.19(A). The resulting stereo photographs from a segment of the west crater wall are shown in Figure 6.19(B), along with an example of the minimum control requirements typically associated with a short aerotriangulated strip. In this case, prominent outcrops and geologic contacts were established as visually identifiable objects in both the aerial photographs and the oblique strips. The rigorous treatment of oblique photography in photogrammetric studies such as this enables precise determination and analysis of 3-D geologic contacts, which record past eruptive and erosive events but typically are not exposed at mid-latitude stratovolcanoes of the northern hemisphere.

Starting in late September 2004, another prolonged episode of dome growth at Mount St. Helens dramatically altered the topographic configuration of the 1980 crater. By March 2005, more than 40×10^6 m^3 of gas-poor, crystal-rich dacite lava had extruded onto the crater floor immediately south of the 1980–1986 dome. The new glacier in the crater was intensely deformed and eventually cut in two by the encroaching dome, resulting in spectacular crevassing and rapid advance of the east arm of the glacier (Figure 6.20) .

Not surprisingly, photogrammetry is playing a

[5] Dome growth resumed in September 2004 and was continuing when this chapter went to press in January 2006.

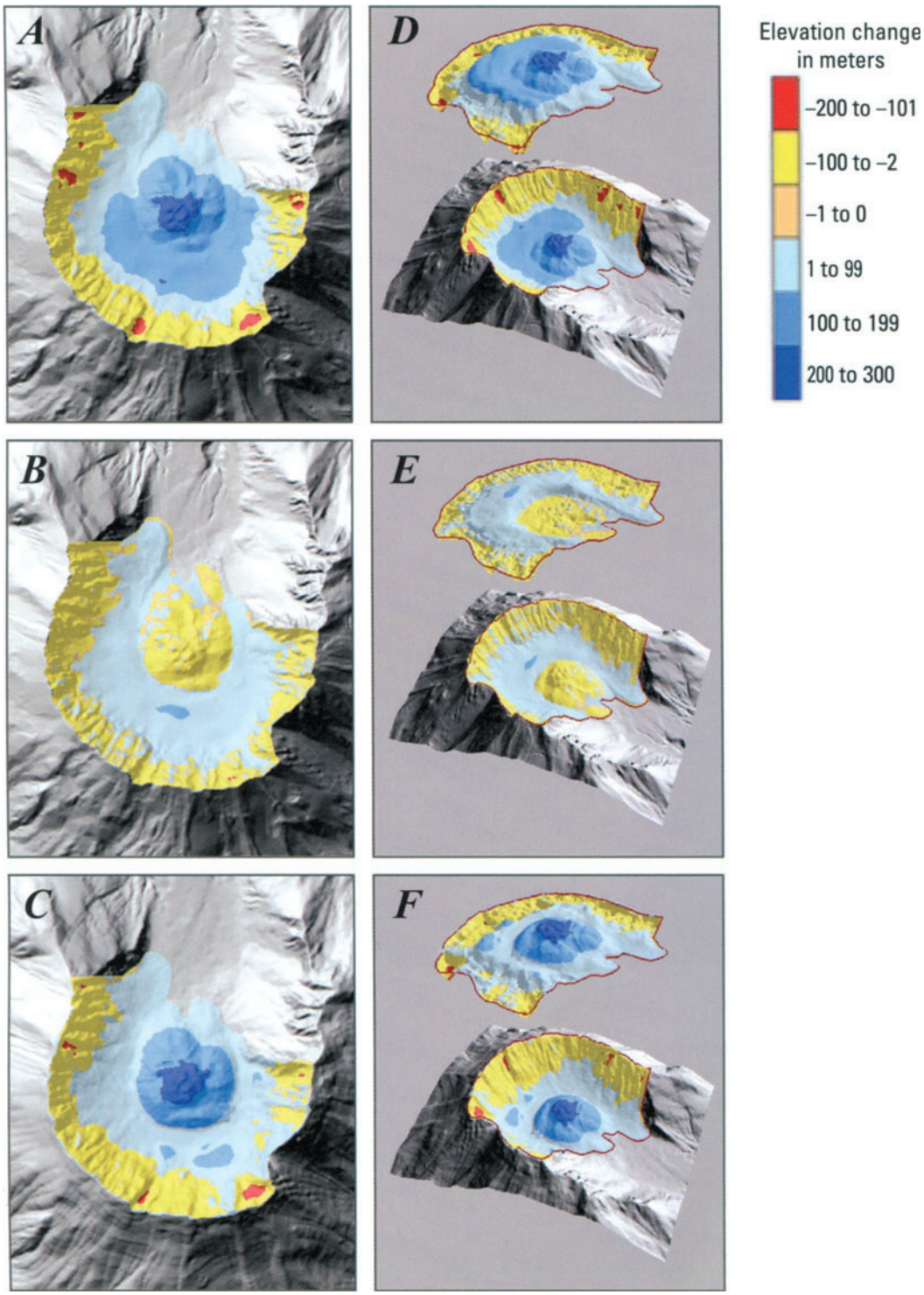

Figure 6.18. Figures 6.18(A–C) show isopach maps, color-coded according to elevation change, for Mount St. Helens derived by: (A) differencing 2000 and 1980 DEMs and draping on the 2000 DEM; (B) differencing 2000 and 1989 DEMs and draping on the 2000 DEM; (C) differencing 1989 and 1980 DEMs and draping on the 1989 DEM. Figures 6.18(D–F) show perspective views from northeast of the same color-coded isopach maps draped over the same shaded relief maps as in (A–C). Above each shaded relief map in (D–F) is a shaded isopach surface color-coded according to thickness (i.e., the floating surfaces represent elevation *changes* during 1980–2000 (D), 1989–2000 (E), and 1980–1989 (F). Negative isopach values indicate erosion, subsidence, or both. Positive isopach values indicate deposition, uplift, or both. See text for discussion. Cell size for the DEMs is 10 meters.

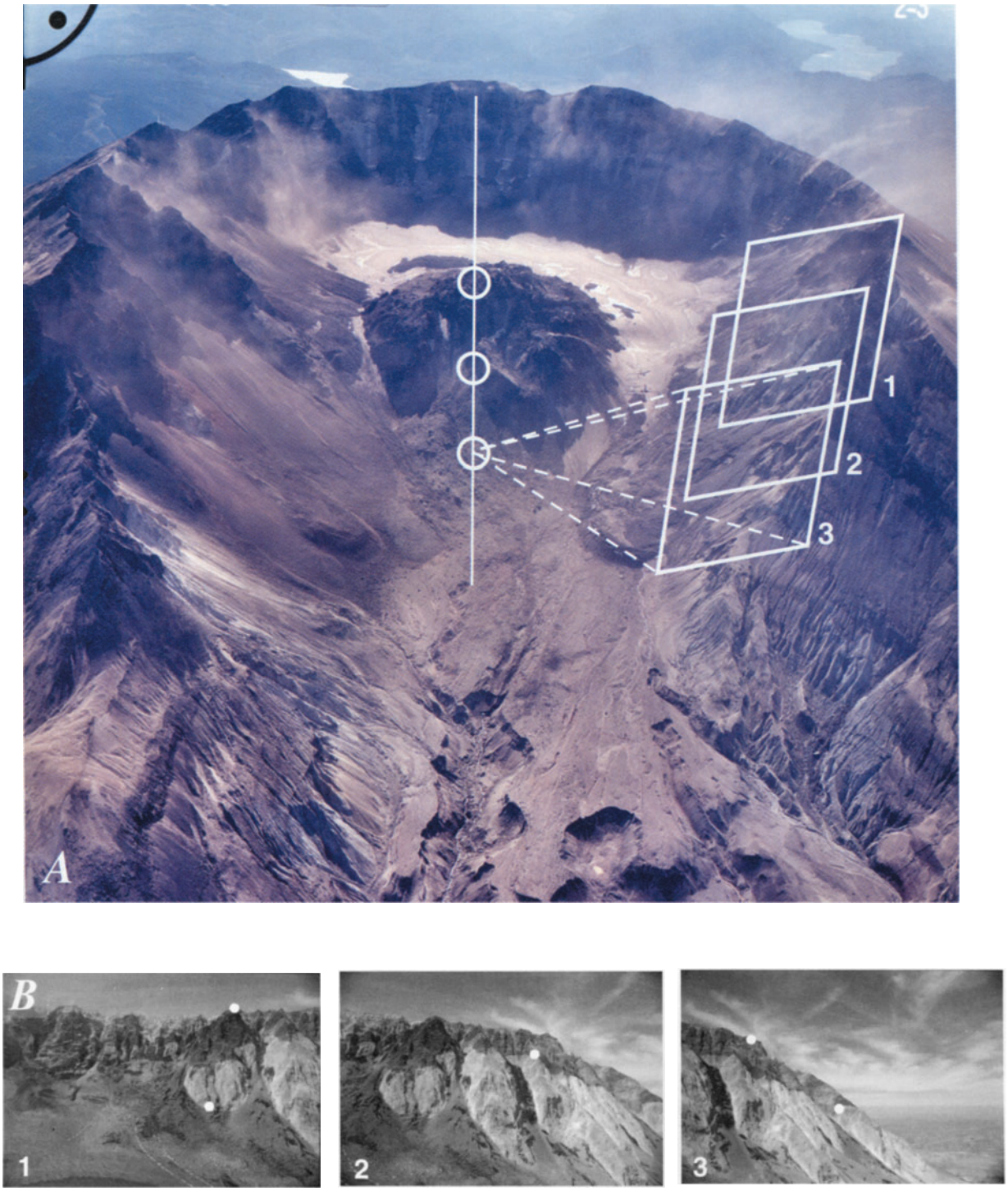

Figure 6.19. (A) Oblique view southward into Mount St. Helens crater showing approximate orientation of N–S flight line used to collect oblique stereo photography of the east and west crater walls. This photograph was acquired on standard 230-mm (9-inch) film with a metric camera and a relatively long focal length (305-mm, 12-inch) lens (noted at top-right edge of photo), which provided a 56° angular field of view. White panels (1, 2, 3) show approximate coverage of oblique photos shown in (B), which were aquired with a small-format (35-mm) non-metric camera and a 28-mm wide-angle lens. (B) Small format (24 mm × 36 mm) stereo photographs of Mount St. Helens' west crater wall with relative positions shown in (A). White dots indicate minimum control point configuration used to orient the oblique photo strip. Coordinate locations of control points were transferred from September 2000 aerial photography (1 : 12,000 scale).

Figure 6.20. The 1980 crater at Mount St. Helens as it appeared on 11 March 2005. View is to the southwest; north is to the lower right in the photo. A lava dome that grew episodically from 1980 to 1986 had been surrounded on three sides and partly buried by a combination of rockfall talus from the crater walls and perennial ice, which persisted owing to the shadowing effect of the steep crater walls and to insulation by annual (summer) talus layers. The rock-and-ice glacier, which was thickest south of the 1980–1986 dome, moved northward around the dome's east and west flanks. The 2004–2005 lava dome issued from a southward-inclined vent near the south margin of the older dome, severely disrupting the thickest part of the glacier on the south crater floor. The east arm of the glacier, which was pushed eastward and upward by the growing dome, became deeply crevassed and its northward motion accelerated dramatically. Dark material on the east arm of the glacier and east crater wall is airfall ash lofted by a small explosive event on 8 March 2005. USGS photograph by Steve P. Schilling.

key role in documenting and interpreting this latest activity. Both conventional 9×9-inch vertical aerial photographs and small-format oblique stereo photographs of the growing dome are being acquired at 2–4 week intervals, the latter from a helicopter using a digital SLR camera with a calibrated lens. The oblique photos are particularly useful for extending stereo coverage into areas that are obscured in some of the vertical photos by clouds, deep shadows, or a persistent eruption plume. High-resolution (2-m cell size) DEMs are being produced from the photos within several days to a few weeks, depending on the urgency of the situation and area of interest. The entire 1980 crater is included in each set of vertical or oblique photos, but the area of interest for DEM construction varies. Should the area of interest increase in the future (e.g., as the dome grows or more of the glacier is deformed), the DEMs for past epochs can be extended using a digital photo archive – an efficient and cost-effective approach. The resulting archive of digital photographs and 3-D terrain models is likely to be the most detailed ever assembled during a dome-building eruption, and it constitutes a valuable resource for current and future investigators.

Clearly, photogrammetry has earned its place among other geodetic techniques in the modern volcanologist's tool kit. As digital SLRs become more affordable and widely available, and softcopy stereoplotters become more generally accessible, the analytical power of photogrammetry will extend to many of the world's deforming volcanoes. Great care still will be required, both in the field and on the stereoplotter, to produce optimal results. But the potential exists for legions of geologists, seismologists, geochemists, and others – already armed with digital cameras – to serve the cause of volcano geodesy. Now, *that's* exciting!